Molecular Pharmacology Fast Forward. Published on April 19, 2010 as doi:10.1124/mol.110.064584

Mapping the binding pocket of dual antagonist almorexant to human orexin 1 and orexin 2 receptors: Comparison with the selective OX_1 (SB-674042) and OX_2 (EMPA) antagonists

Pari Malherbe, Olivier Roche, Anne Marcuz, Claudia Kratzeisen, Joseph G. Wettstein, and Caterina Bissantz

Psychiatry Disease area (P.M., A.M., C.K., J.G.W.) and Chemistry Discovery (O.R., C.B.), F. Hoffmann-La Roche Ltd., CH-4070 Basel, Switzerland

Molecular Pharmacology Fast Forward. Published on April 19, 2010 as DOI: 10.1124/mol.110.064584
This article has not been copyedited and formatted. The final version may differ from this version.

Running title: Mapping binding site of orexin receptor antagonists

Address correspondence to: Dr. Pari Malherbe, F. Hoffmann-La Roche Ltd., Bldg. 69/333, CH-4070 Basel, Switzerland. Tel: +41-61-688-6286; Fax: + 41-61-688-1720; E-mail: parichehr.malherbe@roche.com

Number of text page: 29

Number of tables: 5

Number of figures: 7

Number of references: 38

Number of words in the Abstract: 252

Number of words in the Introduction: 751

Number of words in the Discussion: 1502

Abbreviations: OX, orexin receptor; OX_1, orexin 1 receptor; OX_2, orexin 2 receptor; almorexant, (2*R*)-2-{(1*S*)-6,7-Dimethoxy-1-[2-(4-trifluoromethyl-phenyl)-ethyl]-3,4-dihydro-1H-isoquinolin-2-yl}-*N*-methyl-2-phenyl-acetamide; EMPA, *N*-Ethyl-2-[(6-methoxy-pyridin-3-yl)-(toluene-2-sulfonyl)-amino]-*N*-pyridin-3-ylmethyl-acetamide; SB-674042, 1-(5-(2-fluoro-phenyl)-2-methyl-thiazol-4-yl)-1-((S)-2-(5-phenyl-(1,3,4)oxadiazol-2-ylmethyl)-pyrrolidin-1-yl)-methanone; GPCRs, G-protein coupled receptors; 3D, three-dimensional; 7TMD, seven-transmembrane domain; $[Ca^{2+}]_i$, cytosolic free Ca^{2+} concentration; FLIPR, Fluorometric Imaging Plate Reader; OPSD, bovine rhodopsin; β_2AR, β2-adrenergic receptor; A_{2A}, A_{2A} adenosine receptor; WT, wild type; NK, neurokinin; NK_3, neurokinin 3 receptor; V_1, vasopressin 1 receptor

Molecular Pharmacology Fast Forward. Published on April 19, 2010 as DOI: 10.1124/mol.110.064584
This article has not been copyedited and formatted. The final version may differ from this version.

Abstract

The orexins and their receptors are involved in the regulation of arousal and sleep–wake cycle. Clinical investigation with almorexant has indicated that this dual OX antagonist is efficacious in inducing and maintaining sleep. Using site-directed mutagenesis, β_2-adrenergic-based OX_1 and OX_2 modeling, we have determined important molecular determinants of the ligand-binding pocket of OX_1 and OX_2. The conserved residues $D^{45.51}$, $W^{45.54}$, $Y^{5.38}$, $F^{5.42}$, $Y^{5.47}$, $Y^{6.48}$ and $H^{7.39}$ were found to be contributing to both orexin-A-binding sites at OX_1 and OX_2. Among these critical residues, five (positions 45.51, 45.54, 5.38, 5.42 and 7.39) were located on the ECL2b and in the top of TM domains at the interface to the main binding crevice, thereby suggesting superficial OX receptor interactions of orexin-A. We found that the mutations $W214A^{45.54}$, $Y223A^{5.38}$, $F227A^{5.42}$, $Y317A^{6.48}$ and $H350A^{7.39}$ resulted in the complete loss of both [^{3}H]almorexant and [^{3}H]EMPA binding affinities and also blocked their inhibition of orexin-A-evoked $[Ca^{2+}]_i$ response at OX_2. The crucial residues $Q126^{3.32}$, $A127^{3.33}$, $W206^{45.54}$, $Y215^{5.38}$, $F219^{5.42}$ and $H344^{7.39}$ are shared between almorexant and SB-674042 binding sites in OX_1. The non-conserved residue at position 3.33 of orexin receptors was identified as occupying a critical position that must be involved in subtype selectivity and also in differentiating two different antagonists for the same receptor. In summary, despite high similarities in the ligand-binding pockets of OX_1 and OX_2 and numerous aromatic/hydrophobic interactions, the local conformation of helix positions 3.32, 3.33 and 3.36 in TM3 and 45.51 in ECL2b provide the structural basis for pharmacologic selectivity between OX_1 and OX_2.

Molecular Pharmacology Fast Forward. Published on April 19, 2010 as DOI: 10.1124/mol.110.064584
This article has not been copyedited and formatted. The final version may differ from this version.

Introduction

Hypothalamic neuropeptides, orexin-A/hypocretin-1 (33 amino acids) and orexin-B/hypocretin-2 (28 amino acids), are derived from the proteolytic processing of 130 amino acids prepro-orexin (de Lecea et al., 1998; Sakurai et al., 1998). Orexin peptides elicit their effect through two G-protein-coupled receptors (GPCRs) called OX_1 and OX_2 (nomenclature follows Alexander et al., 2008) that couple to $G_{q/11}$ and contribute to the activation of phospholipase C, leading to the elevation of intracellular Ca^{2+} concentrations (Sakurai et al., 1998). However, a detailed signaling profile of the hOX_2 has recently shown that OX_2 could couple to Gs as well as $G_{q/11}$ and G_i pathways (Tang et al., 2008). The binding and functional characterization demonstrated that orexin-B has a 10-fold lower affinity for the OX_1 over the OX_2, while both orexin-A and orexin-B bind with similar affinities to OX_2 (Sakurai et al., 1998).

Distribution studies in rat brain using in situ hybridization and immunohistochemistry have shown that orexin neurons are found exclusively in the lateral hypothalamic area, having projections to the entire CNS (Nambu et al., 1999; Peyron et al., 1998). OX_1 and OX_2 receptors are differentially expressed in the CNS. Although both receptors are present in most brain regions such as neocortex L6, ventral tegmental area, preoptic area, dorsal and medial raphe nuclei, periaqueductal area and hypothalamus, OX_1 is most abundantly expressed in the locus coeruleus while OX_2 is expressed in regions controlling arousal, especially in the tuberomammillary nucleus, an important site for the regulation of sleep/wakefulness (Marcus et al., 2001; Trivedi et al., 1998).

Orexin system has been implicated in numerous physiological functions including energy homeostasis, feeding and reward, also regulation of arousal and the sleep–wake cycle (Kilduff and Peyron, 2000; Ohno and Sakurai, 2008). Preclinical (canine and rat) and Clinical (healthy male subjects; single dose) investigations have shown that almorexant, when

Molecular Pharmacology Fast Forward. Published on April 19, 2010 as DOI: 10.1124/mol.110.064584
This article has not been copyedited and formatted. The final version may differ from this version.

administered orally during the active period, promoted sleep in animals and humans without disrupting the sleep architecture or inducing cataplexy (Brisbare-Roch et al., 2007; Neubauer, 2010), thereby further validating the involvement of orexin system in the regulation of alertness and sleep. Thus, OX antagonists represent an alternative therapeutical approach for the treatment of insomnia (Boss et al., 2009; Nishino, 2007; Roecker and Coleman, 2008). Recently, the biochemical characterization of a high-affinity, reversible and *in vivo* active OX_2 antagonist, EMPA, with 900-fold selectivity in binding for OX_2 over OX_1 has been reported (Malherbe et al., 2009a). Furthermore, the biochemical characterization of almorexant (a high-affinity dual OX_1/OX_2) has demonstrated that it had an apparent non-competitive and long-lasting pseudo-irreversible mode of antagonism due to its very slow rate of dissociation from OX_2, whereas it displayed a competitive mode of antagonism at OX_1 (Malherbe et al., 2009b). SB-674042, which is a high-affinity and selective OX_1 antagonist (Langmead et al., 2004), has been also shown to behave in an apparent non-competitive manner at hOX_1, similarly to that of almorexant at hOX_2 (Malherbe et al., 2009b).

Several researchers, who have investigated the determinants of orexin-A required to activate OX_1 and OX_2 using truncated peptides and alanine-scanned peptides (systematic replacement of the natural amino acids with L-alanine) (Ammoun et al., 2003; Lang et al., 2006; Lang et al., 2004; Takai et al., 2006) have indicated that: (1) a minimal 19 amino acids of C-terminal segment of orexin-A (R15-L33) is required for OX activation, though functional activity of this peptide is reduced; (2) the replacement of orexin-A (R15–L33) truncated peptide residues, Leu16, Leu19, Leu20, His26, Gly29, Ile30, Leu31, Thr32, and Leu33 with alanine led to a significant reduction in the functional potency at the OX_1 (Darker et al., 2001); and (3) orexin-A distinctly recognized OX_1 from OX_2 and its binding to OX_1 required more molecular determinants than binding to OX_2. Thus far, little is known about OX ligand-binding pocket. The current research utilized a combination of β2AR-based OX_1

Molecular Pharmacology Fast Forward. Published on April 19, 2010 as DOI: 10.1124/mol.110.064584
This article has not been copyedited and formatted. The final version may differ from this version.

and OX_2 modeling, site-directed mutagenesis, [^{3}H]almorxant, [^{3}H]EMPA and [^{3}H]SB-674042 bindings and orexin-A evoked intracellular calcium ($[Ca^{2+}]_i$) mobilization (FLIPR) assay to probe the antagonist-binding site of OX_1 and OX_2. Amino acid residues in the TM3, -5, -6 and -7 and ECL2b regions, initially identified from an alignment of the 7TMD of OX_1 and OX_2 with hβ2AR were demonstrated by mutational analysis to be important determinants of the high-affinity antagonist-binding pocket of the OX_1 and OX_2. Furthermore, these experimental findings allow the construction of homology models of OX_1– and OX_2–7TMD based on the X-ray crystal of hβAR (2RH1) (Cherezov et al., 2007; Rosenbaum et al., 2007) and suggest possible binding modes for EMPA–OX_2, SB-674042–OX_1, and almorexant–OX_1 and –OX_2 complexes.

Molecular Pharmacology Fast Forward. Published on April 19, 2010 as DOI: 10.1124/mol.110.064584
This article has not been copyedited and formatted. The final version may differ from this version.

Materials and Methods

Materials. Almorexant (ACT-078573) (Brisbare-Roch et al., 2007), EMPA (Malherbe et al., 2009a), and SB-674042 (Langmead et al., 2004) were synthesized in the Chemistry Department of F. Hoffmann-La Roche. [^{3}H]almorexant (specific activity: 42.7 Ci/mmol), [^{3}H]EMPA (specific activity: 94.3 Ci/mmol) and [^{3}H]SB-674042 (specific activity: 24.4 Ci/mmol) (**Fig. 1A**) were synthesized by Drs. Philipp Huguenin and Thomas Hartung at the Roche chemical and isotope laboratories, Basel, Switzerland. orexin-A (**Fig. 1B**) was purchased from Tocris Bioscience (Bristol, UK).

Construction of point-mutated hOX_1 and hOX_2 receptors. cDNA encoding human OX_1 (Accession No. O43613) and human OX_2 (Accession No. O43614) were subcloned into pCI-Neo expression vectors (Promega, Madison, WI). All point-mutants were constructed using the QuikChange^{TM} site-directed mutagenesis kit (Stratagene, La Jolla, CA) according to the manufacturer's instructions and using pCI-Neo-hOX_1 or pCI-Neo-hOX_2 as a DNA template. Complementary oligonucleotide primers (sense and antisense) containing the single site of mutation was synthesized by Microsynth AG (Balgach, Switzerland). The following PCR conditions were used for repeated extensions of the plasmid template: 95°C for 1 min and 20 cycles of 95°C for 30 s, 55°C for 1 min and 68°C for 8 min using 50 ng plasmid DNA, 100 ng each of primers and 2.5 units Pfu Turbo DNA polymerase (Stratagene). The entire coding regions of all positive point-mutants were sequenced from both strands using an automated cycle sequencer (Applied Biosystems).

Cell culture and membrane preparation. HEK293 cells were transfected as previously described (Malherbe et al., 2009a). Forty-eight hours after transfection, cells were harvested and washed three times with cold phosphate-buffered saline and frozen at –80°C. The pellet was suspended in ice-cold buffer containing 15 mM Tris-HCl, pH 7.5, 2 mM $MgCl_2$, 0.3 mM EDTA, 1 mM EGTA, protease inhibitor cocktail EDTA-free (Roche Applied

Molecular Pharmacology Fast Forward. Published on April 19, 2010 as DOI: 10.1124/mol.110.064584
This article has not been copyedited and formatted. The final version may differ from this version.

Science, RAS, Rotkreuz, Switzerland) and homogenized with a polytron (Kinematica AG, Basel, Switzerland) for 30 s at 16 000 rpm. After centrifugation at 48 000 X g for 30 min at 4°C, the pellet was suspended in ice-cold buffer containing 75 mM Tris-HCl, pH 7.5, 12.5 mM $MgCl_2$, 0.3 mM EDTA, 1 mM EGTA, 250 mM sucrose, protease inhibitor cocktail EDTA-free. The membrane homogenate was frozen at –80°C before use.

[^{3}H]almorexant, [^{3}H]EMPA and [^{3}H]SB-674042 bindings. After thawing, membrane homogenates were centrifuged at 48 000 X g for 10 min at 4°C, the pellets were resuspended in the binding buffer (1 X HBSS, 20 mM HEPES, pH 7.4, 0.1% BSA) to a final assay concentration of 5 µg protein/well. Saturation isotherms were determined by addition of various concentrations of [^{3}H]almorexant (0.02-20 nM at OX_1, 0.03-15 nM at OX_2R), [^{3}H]EMPA (0.01 to 12 nM at OX_2) or [^{3}H]SB-674042 (0.03-15 nM at OX_1) to these membranes (in a total reaction volume of 500 µl). The incubation time for [^{3}H]almorexant and [^{3}H]SB-674042 on OX_1 membranes was 90 min at 23°C. The incubation for [^{3}H]almorexant and [^{3}H]EMPA on OX_2 expressing membrane was 120 min and 60 min at 23°C, respectively. At the end of incubation, membranes were filtered onto unitfilter (96-well white microplate with bonded GF/C filter pre-incubated for 1 h in wash buffer plus 0.5% polyethylenimine and 0.1% BSA) with a Filtermate 196 harvester (PerkinElmer Life and Analytical Sciences, Waltham, MA) and washed four times with ice-cold wash buffer (1 X HBSS, 20 mM HEPES, pH 7.4). Nonspecific bindings for [^{3}H]almorexant, [^{3}H]EMPA and [^{3}H]SB-674042 were measured in the presence of 10 µM almorexant, EMPA and SB-674042, respectively. Radioactivity on the filter was counted (5 min) on a Top-Count microplate scintillation counter (PerkinElmer Life and Analytical Sciences) with quenching correction after addition of 45 µl of microscint 40 (PerkinElmer Life and Analytical Sciences) and shaking for 1 h. Saturation experiments were analyzed by Prism 5.0 (GraphPad software, San Diego, CA) using the rectangular hyperbolic equation derived from the equation of a

Molecular Pharmacology Fast Forward. Published on April 19, 2010 as DOI: 10.1124/mol.110.064584
This article has not been copyedited and formatted. The final version may differ from this version.

bimolecular reaction and the law of mass action, $B = (B_{max} * [F])/(K_d + [F])$, where B is the amount of ligand bound at equilibrium, B_{max} is the maximum number of binding sites, [F] is the concentration of free ligand and K_d is the ligand dissociation constant**.** For all mutants, the experiments were performed three to five times in triplicate and the mean ± SE of the individual K_d and Bmax values were calculated and are reported. Statistical significance was determined using the Two-tailed t-test (Prism 5.0, GraphPad software).

Intracellular Ca^{2+} mobilization, $[Ca^{2+}]_i$ assay. HEK293 cells, which were grown to 80% confluency in growth medium (DMEM high glucose supplemented with 10% fetal calf serum and 100 µg/µl penicillin/streptomycin), were transfected with the wild type or mutant orexin receptor cDNAs in pCI-Neo using Lipofectamine Plus™ reagent (Invitrogen, Carlsbad, CA) according to the manufacturer's instruction. Six hours after transfection, the DNA-transfection mixture was removed and the cells were maintained in growth medium. Twenty four hours after transfection,, the cells were harvested and seeded at $6x10^4$ cells/well in the poly-D-lysine treated, 96-well, black/clear-bottomed plates (BD Biosciences, Palo Alto, CA). Forty-eight hours after transfection, the cells were loaded for 1h at 37°C with 4 µM Flou-4AM (Molecular Probes, Eugene, OR) in loading buffer (1xHBSS, 20 mM HEPES). The cells were washed five times with loading buffer to remove excess dye and intracellular calcium mobilization, $[Ca^{2+}]_i$ were measured using a Fluorometric Imaging Plate Reader (FLIPR, Molecular Devices, Menlo Park, CA) as described previously (Malherbe et al., 2009b). Orexin-A (50 mM stock solution in DMSO) was diluted in FLIPR buffer plus 0.1% BSA. The EC_{50} and EC_{80} values of orexin-A were measured daily from standard agonist concentration-response curves in HEK293 cells transiently transfected with the WT or mutant orexin receptors. Inhibition curves were determined by addition of 11 concentrations (0.0001-10 µM in FILPR buffer) of inhibitory compounds and using EC_{80} value of orexin-A as agonist (a concentration which gave 80% of maximum agonist response, determined daily). The

Molecular Pharmacology Fast Forward. Published on April 19, 2010 as DOI: 10.1124/mol.110.064584
This article has not been copyedited and formatted. The final version may differ from this version.

antagonists were applied 25 min (incubation at 37°C) before the application of the agonist. Responses were measured as peak increase in fluorescence minus basal, normalized to the maximal stimulatory effect induced by EC_{80} value of orexin-A. Inhibition curves were fitted according to the Hill equation: $y = 100/(1+(x/IC_{50})^{nH})$, where n_H = slope factor using Prism 5.0 (GraphPad software). K_b values were calculated according to the following equation $K_b = IC_{50}/(1+[A]/EC_{50})$, where A is the concentration of agonist added that is very close to agonist EC_{80} value, and IC_{50} and EC_{50} values were derived from the antagonist inhibition and orexin agonist curves, respectively. The relative efficacy (E_{max}) values of orexin-A was calculated as fitted maximum of the dose-response curve of each mutated receptors expressed as a percentage of fitted maximum of the wild type dose-response curve from cells transfected and assayed on the same day.

Residue Numbering Scheme

The position of each amino acid residue in the seven membrane domain (7TMD) was identified both by its sequence number and by its generic number proposed by Ballesteros and Weinstein (Ballesteros and Weinstein, 1995). In this numbering system, amino acid residues in the 7TMD are given two numbers; the first one refers to the transmembrane (TM) number (1-7), the second one indicates the relative position relative to a highly conserved residue in class A GPCRs in that TM, which is arbitrarily assigned 50. The second extracellular loop (ECL2) is labeled 45 to indicate its location between helices 4 and 5 and the conserved cysteine thought to be disulfide bonded, is given index number 45.50. The residues within ECL2 loop are then indexed relative to this position. ECL2b is the C-terminal strand of ECL2, which connects $C^{3.25}$ with $C^{45.50}$.

Alignment and model building. The amino acid sequences of the human OX_1 (O43613), human OX_2 (O43614) were retrieved from the Swiss-Prot database. A model was built by aligning the 7 TMs and ECL2 of orexin receptor sequences on the β2-adrenergic

receptor (P07550) sequence to use the 2.4 Å high resolution crystal structure determined by Cherezov *et al* as a template (the PDB structure 2RH1, Cherezov et al., 2007; Rosenbaum et al., 2007). The initial alignment was generated with the clustalW multiple alignment program using the BLOSUM matrix and then manual inspection was performed to ensure that conserved residues were aligned. Then, the software package MOE (MOE version 2005.05; Chemical Computing Group, Montreal, Quebec, QC, Canada) was used to create 3D models of human OX_1 and OX_2 either based on β2-adrenergic (2RH1). Ten intermediates were generated and the best model was selected. No minimization was performed to keep the backbone coordinates of the crystallographic structure. The three molecules (SB-674042, EMPA and almorexant) were then manually docked into the membrane cavity. The binding site was defined as the set of amino acids found at 6.0Å away from the carazolol in the X-ray structure of β2-adrenergic receptor.

Molecular Pharmacology Fast Forward. Published on April 19, 2010 as DOI: 10.1124/mol.110.064584
This article has not been copyedited and formatted. The final version may differ from this version.

Results

Binding characteristics of [^{3}H]SB-674042, [^{3}H]EMPA and [^{3}H]almorexant. To investigate 7TMD pocket of OX_1 and OX_2 receptors, three radioligand antagonists; [^{3}H]SB-674042, [^{3}H]EMPA and [^{3}H]almorexant were selected for current study (**Fig. 1A**). [^{3}H]SB-674042 is the first radioligand antagonist selective for hOX_1 to be described (Langmead et al., 2004). In the filtration binding assay, [^{3}H]SB-674042 has displayed a high affinity binding to hOX_1 with a K_d value of 0.74 nM. SB-674042 has also showed a 275-fold selectivity in functional assay (FLIPR) for hOX_1 over hOX_2 (Malherbe et al., 2009b). Recently, the biochemical characterization of an OX_2 antagonist, EMPA, with 900-fold selectivity in binding for OX_2 over OX_1 has been reported (Malherbe et al., 2009a). [^{3}H]EMPA is a high affinity radioligand that binds to HEK293-hOX_2 membrane with K_d value of 1.1 nM. [^{3}H]almorexant bound with high affinity to a single saturable site on recombinant hOX_1 and hOX_2 with K_d values of 1.3 nM and 0.17 nM, at 37ºC, respectively (Malherbe et al., 2009b). Furthermore, SB-674042 and EMPA were able to displace the [^{3}H]almorexant binding from hOX_1 and hOX_2 membranes with K_i values of 1.9 nM and 1.2 nM, respectively. Therefore, it is concluded that almorexant should share a common binding pocket in the transmembrane region of the orexin receptors or at least overlapping with those of SB-674042 on hOX_1 and EMPA on hOX_2.

Alignment of 7TM domains of the OX receptors towards hβ2AR and selection of the orexin receptor mutations. The orexin receptors are highly conserved across mammalian species. Human OX_1 and OX_2 display 64% overall sequence identity (Sakurai et al., 1998), an even higher degree of identity of 84% is found when comparing 7TMD regions (**Fig. 2**). To elucidate the binding modes of almorexant, EMPA and SB-674042, an alignment of the seven transmembrane helices of the hOX_1 and hOX_2 towards the transmembrane helices of human β2-adrenergic receptor (PDB ref code 2RH1) (Cherezov et al., 2007; Rosenbaum et al., 2007)

Molecular Pharmacology Fast Forward. Published on April 19, 2010 as DOI: 10.1124/mol.110.064584
This article has not been copyedited and formatted. The final version may differ from this version.

was made (**Fig. 3**). In **Fig. 3**, an alignment of 7TM of the hOX_1 and hOX_2 towards the 7TM of bovine rhodopsin (PDB ref code 1F88) (Palczewski et al., 2000) and human A_{2A} adenosine receptor (PDB ref code 3EML) (Jaakola et al., 2008) were also shown for comparison. Since at early stage of current study, OX_2 was our target, the first site directed mutagenesis campaign has focused on the elucidation of the binding mode of the selective hOX_2 EMPA (Malherbe et al., 2009a) and the dual acting molecule almorexant (Malherbe et al., 2009b) against the human orexin 2 receptor. The partial inverse agonist of human β2-adrenergic receptor, carazolol, was employed as a template for the locations of EMPA and almorexant. Amino acids, which were found 6.0 Å away from carazolol in the X-ray crystal structure of β2-adrenergic receptor (Cherezov et al., 2007; Rosenbaum et al., 2007), were generally considered as possible candidates to affect bindings of EMPA and almorexant. **Fig. 3** shows a set of 17 mutations covering the whole binding site (TM2, -3, -5, -6, -7 and ECL2b) that was suggested from the manual docking of almorexant in the hOX_2 3D homology model. Seventeen residues of OX_2 were mutated to alanine and OX_2 $Y317^{6.48}$ was additionally mutated to Phenylalanine to discriminate between its aromatic and hydrogen bond donor capabilities. For OX_1, we selected a smaller list of residues that had been proven to be important for OX_2. Ten residues of OX_1 were mutated to alanine and OX_1 $A127^{3.33}$ was changed to threonine to mimic the OX_2 residue (**Fig. 3**). Overall, twenty-nine point-mutations, eighteen in hOX_2 and eleven in hOX_1 were accordingly introduced in the 7TMD region by site-directed mutagenesis.

Effect of mutations on hOX_1- or hOX_2-mediated of orexin-A-evoked $[Ca^{2+}]_i$ response. In HEK293 cells transiently expressing hOX_1 or hOX_2, orexin-A (0.0001-10 μM) elicited a concentration-dependent increase in intracellular free calcium $[Ca^{2+}]_i$ as monitored using the Ca^{2+}-sensitive dye Flou-4 and a Fluorometric Imaging Plate Reader (FLIPR-96). As seen in **Table 1** and **Table 2**, orexin-A activates hOX_2 and hOX_1 with similar potency.

Molecular Pharmacology Fast Forward. Published on April 19, 2010 as DOI: 10.1124/mol.110.064584
This article has not been copyedited and formatted. The final version may differ from this version.

The EC_{50}, n_H and relative E_{max} values, calculated from concentration-response curves of orexin-A in the cells expressing WT and mutated hOX_2 receptors, are given in **Table 1**. The mutations T111A$^{2.61}$, D211A$^{45.51}$, W214A$^{5.54}$, Y223A$^{5.38}$, F227A$^{5.42}$, F346A$^{7.35}$ and H350A$^{7.39}$ caused a large decrease in the potency of orexin-A (by 243.5-, 416.1-, 62.4-, 183.9-, 240.3-, 54.5- and 49.5-fold) respectively, without affecting their efficacy, in comparison to the WT. The mutations Y232A$^{5.47}$ and Y317A$^{6.48}$ resulted in a moderate reduction of both potency (by 28.4-and 17.7-fold) and efficacy (relative E_{max} of 44.9% and 49.6%) of orexin-A, respectively. The mutation Q134A$^{3.32}$ caused a moderate decrease in potency of orexin-A (by 22.3-fold) without having effect on its efficacy.

The effect of mutations on potency (EC_{50}) and efficacy (relative E_{max}) of orexin-A in the HEK293 cells transiently expressing WT and mutated hOX_1 receptors, are given in **Table 2**. The mutations D203A$^{45.51}$, W206A$^{45.54}$, Y215A$^{5.38}$, F219A$^{5.42}$, Y224A$^{5.47}$, Y311A$^{6.48}$ and H344A$^{7.39}$ caused large decreases in the potency of orexin-A (by 408.2-, 417.8-, 407.8-, 139.6-, 84.4-, 163.9- and 241.1-fold), in comparison to the WT. Except for the mutation of W206A$^{45.54}$, which caused a moderate decrease of orexin-A's efficacy (relative E_{max} of 45.0%), other mutations had no major effect on efficacy of orexin-A. The mutation V130A$^{3.36}$ affected moderately the potency of orexin-A (30.6-fold), without having any effect on its efficacy.

Effect of mutations on binding affinity and function potency of [^{3}H]EMPA and [^{3}H]almorexant at OX_2 receptor. To characterize the binding pockets of EMPA and almorexant, 18 point-mutations located in theTM2, -3, -5, -6, and -7 and ECL2b regions of hOX_2, were selected based on proposed docking mode of almorexant (**Fig. 3**). With the exception of the Y232A$^{5.47}$ and Y317A$^{6.48}$, which produced a reduction in orexin-A-stimulated fluorescence responses in the FLIPR experiment, the 16 mutations had no effect on or partially affected the orexin-A-induced FLIPR signal. Saturation binding analyses were

Molecular Pharmacology Fast Forward. Published on April 19, 2010 as DOI: 10.1124/mol.110.064584
This article has not been copyedited and formatted. The final version may differ from this version.

performed on membranes isolated from the HEK293 transiently transfected with the WT and mutated hOX_2 receptors using 0.01 to 12 nM concentrations of [^{3}H]EMPA or 0.03 to 15 nM concentrations of [^{3}H]almorexant. The dissociation constants (K_d) and the maximum binding sites (B_{max}) derived from the saturation isotherms are given in **Table 3**.

The mutations T135A$^{3.33}$, W214A$^{45.54}$, Y223A$^{5.38}$, F227A$^{5.42}$, Y232A$^{5.47}$, Y317A$^{6.48}$, I320A$^{6.51}$, H350A$^{7.39}$ and Y354A$^{7.43}$, abolished [^{3}H]EMPA binding to undetectable levels (K_d>30 nM can not be detected because of high non-specific binding, NSB>SB). The binding affinity of [^{3}H]EMPA was decreased by 7.4-, 14.9-, 8.7- and 3.9-fold by mutations T111A$^{2.61}$, V138A$^{3.36}$, D211A$^{45.51}$ and Y317F$^{6.48}$, and were statistically significant (P = 0.03, 0.0001, 0.003, 0.002), respectively (**Table 3**). In functional FLIPR assay (**Fig. 4, A, C and E, and Table 3**), in cells expressing the mutants T135A$^{3.33}$, W214A$^{45.54}$, Y223A$^{5.38}$, F227A$^{5.42}$, Y232A$^{5.47}$, Y317A$^{6.48}$, I320A$^{6.51}$, H350A$^{7.39}$ and Y354A$^{7.43}$, that did not bind [^{3}H]EMPA, EMPA was not able to efficiently inhibit orexin-A-evoked $[Ca^{2+}]_i$ response and thus resulted in the large increases in K_b values (2972.7-, >10,000-, 339.0-, 420.0-, 37.1-, 54.5-, 415.5-, 279.1- and 366.4-fold, respectively). The mutations D211A$^{45.51}$ and Y317F$^{6.48}$, which caused the decreases in the EMPA's binding affinity, resulted similarly in decreases of functional potency by 16.8 and 9.5-fold. In general, a good agreement was observed between the effect of mutations on binding affinity and functional potency of EMPA, except for the mutants T111A$^{2.61}$ and V138A$^{3.36}$ in which the effect on functional potency of EMPA was greater than that on binding affinity (51.1- and 90.9-fold increases in K_b values versus 7.4- and 14.9-fold increases in K_d values, respectively).

As seen in **Table 3**, the mutations W214A$^{45.54}$, Y223A$^{5.38}$, F227A$^{5.42}$, Y317A$^{6.48}$ and H350A$^{7.39}$ abolished [^{3}H]almorexant binding to undetectable levels (K_d>20 nM can not be detected because of high non-specific binding, NSB>SB). The binding affinity of [^{3}H]almorexant was decreased by 10.7- and 10.0-fold by mutations Q134A$^{3.32}$ and Y232A$^{5.47}$,

Molecular Pharmacology Fast Forward. Published on April 19, 2010 as DOI: 10.1124/mol.110.064584
This article has not been copyedited and formatted. The final version may differ from this version.

which were statistically significant (P = 0.04 and 0.006), respectively. Interestingly, the mutation F346A$^{7.35}$ caused 3.25-fold increase in affinity of [^{3}H]almorexant with high statistical significant (P = 0.0002). In functional FLIPR assay (**Fig. 4, B, D and F, and Table 3**), in cells expressing the mutants W214A$^{45.54}$, Y223A$^{5.38}$, F227A$^{5.42}$, Y317A$^{6.48}$ and H350A$^{7.39}$ that did not bind [^{3}H]almorexant, almorexant was not able to efficiently inhibit orexin-A-evoked $[Ca^{2+}]_i$ response and thus resulted in the large increases in K_b values (>10,000-, 10,000-, 200.4-, 25.0- and 94.2-fold, respectively). The mutation Y232A$^{5.47}$, which caused a decrease in the almorexant's binding affinity by 10.0-fold, resulted similarly in a decrease of functional potency by 7.5-fold. Therefore, with the exception of mutation Q134A$^{3.32}$, which led to a decrease in binding affinity (10.7-fold) and had no effect on functional potency, a good correlation between binding and functional potency of almorexant was observed at OX_2.

Comparison of mutation effects on binding and functional potencies of SB-674042 and almorexant at OX_1. To determine the residues forming the binding pockets of SB-674042 and almorexant at hOX_1 receptor, 11 point-mutations proposed from docking of almorexant onto OX_1 TM cavity (**Fig. 3**). Saturation binding analyses were performed on membranes isolated from the HEK293 cells transfected with the WT and mutated OX_1 receptors using 0.03 to 15 nM concentrations of [^{3}H]SB-674042 and 0.02-20 nM of [^{3}H]almorexant. The dissociation constants (K_d) and the maximum binding sites (B_{max}) derived from the saturation isotherms are given in **Table 4**. The functional potencies of SB-674042 and almorexant were not measured at D203$^{45.51}$, W206A$^{45.54}$ and Y215A$^{5.38}$ due to high EC_{80} values (>600 nM) of orexin-A.

As seen in the **Table 4**, the mutations W206A$^{45.54}$, Y215A$^{5.38}$ and F219A$^{5.42}$ abolished [^{3}H]SB-674042 binding to undetectable levels (K_d>100 nM can not be detected because of high non-specific binding, NSB>SB). The mutants Q126A$^{3.32}$, A127T$^{3.33}$ and H344A$^{7.39}$

Molecular Pharmacology Fast Forward. Published on April 19, 2010 as DOI: 10.1124/mol.110.064584
This article has not been copyedited and formatted. The final version may differ from this version.

caused dramatic decreases in the binding affinity of [^{3}H]SB-674042 by 50.9-, 20.2- and 22.7-fold, with high statistical significance (P = 0.0005, 0.003 and 0.0005), respectively. The mutations Y311A$^{6.48}$ and Y348A$^{7.43}$ led to decreases in the binding by 10.8- and 9.3-fold, and were statistically significance (P = 0.01 and 0.0003), respectively. In the functional FLIPR assay (**Fig. 5, A and C, and Table 4**), in cells expressing the mutant F219A$^{5.42}$, that did not bind [^{3}H]SB-674042, SB-674042 was not able to efficiently inhibit orexin-A-evoked $[Ca^{2+}]_i$ response and thus resulted in the large increase in K_b value by 311.7-fold. The mutants Q126A$^{3.32}$, A127T$^{3.33}$ and H344A$^{7.39}$ that caused dramatic decreases in the binding affinity of [^{3}H]SB-674042, similarly led to large decreases in functional potency by 40.3-, 22.8- and 20.8-fold, respectively. However, the mutations Y311A$^{6.48}$ and Y348A$^{7.43}$, which led to decreases in the binding affinity of SB-674042, had no effect on its functional potency.

As seen in **Table 4**, the mutations Q126A$^{3.32}$, A127T$^{3.33}$, D203A$^{45.51}$, W206A$^{45.54}$, Y215A$^{5.38}$, F219A$^{5.42}$, Y224A$^{5.47}$, Y311A$^{6.48}$, H344A$^{7.39}$ and Y348A$^{7.43}$ abolished [^{3}H]almorexant binding to undetectable levels (K_d>20 nM can not be detected because of high non-specific binding, NSB>SB). In the functional FLIPR studies (**Fig. 5, B and D, and Table 4**), in cells expressing the mutants Q126A$^{3.32}$, A127T$^{3.33}$, F219A$^{5.42}$, Y311A$^{6.48}$, H344A$^{7.39}$ and Y348A$^{7.43}$ that did not bind [^{3}H]almorexant, almorexant was not able to efficiently inhibit orexin-A-evoked $[Ca^{2+}]_i$ response and thus resulted in the large increases in K_b values (>10,000-, >10,000-, 191.9-, >10,000-, 61.3- and 32.7-fold, respectively). However, the mutation Y224A$^{5.47}$, which caused loss of almorexant's binding affinity, had a marginal effect on its functional potency.

Docking of SB-674042, almorexant and EMPA onto the OX_1–7TMD and OX_2–7TMD binding cavities. Our mutational data indicate that the complexes of antagonists with long-lasting pseudo-irreversible mode of antagonism such as almorexant–OX_2 and SB-674042–OX_1 needed fewer contact sites with the respective receptor, while the complexes of

Molecular Pharmacology Fast Forward. Published on April 19, 2010 as DOI: 10.1124/mol.110.064584
This article has not been copyedited and formatted. The final version may differ from this version.

competitive, reversible antagonists such as EMPA–OX_2 and almorexant–OX_1 were more affected by amino acid replacements, their interactions involving more molecular determinants (**Tables 3 and 4**). To visualize the mutation data, a 3D-model of the hOX_1–7TMD and hOX_2–7TMD using the atomic coordinates of hβ2AR (PDB code, 2RH1) were constructed and three small molecule antagonists docked onto the transmembrane cavity. **Fig. 6A and B** show the docking of almorexant and EMPA to hOX_2. **Fig. 6C** shows both compounds superposed in the hOX_2 binding site. According to the mutational results, both antagonists share important interactions with residues on TM5, -6 and -7. This fits nicely with our predicted docking poses: $Y223^{5.38}$, $F227^{5.42}$ and $Y232^{5.47}$ form a subpocket filled by both antagonists equally well. Also, both almorexant and EMPA can nicely interact with one of their aromatic rings with $H350^{7.39}$ to form an aromatic π-π interaction. Both antagonists are thus docked onto the same region in the homology model. However, due to their singular chemical structures they show different effects with further surrounding residues. Most importantly, only the OX_2 selective ligand EMPA was affected by the $T135A^{3.33}$ mutation. This might be explained by the fact that EMPA is located closer to this residue than almorexant and can form a hydrogen bond with the pyridyl group. Besides, only EMPA was affected by the $V138A^{3.36}$, $Y317F^{6.48}$ and $I320^{6.51}$ mutations. As **Fig. 6B/C** shows, these four residues are located closely to each other deep in the binding cavity and are forming a subpocket filled with the para-methoxy substituted pyridyl group of EMPA. Almorexant, on the other side, does not reach as deep into this part of the pocket and is thus not influenced by these three mutations. The effect of $F346A^{7.35}$ on only almorexant can be explained by the suboptimal geometry of the edge-to-face aromatic interaction of the phenyl substituent of almorexant with $F346^{7.35}$: The aromatic hydrogens of the phenyl substituent of almorexant point onto the aromatic hydrogens of $F346^{7.35}$ rather than onto the aromatic face. This is an unfavorable situation. Consequently, removal of the aromatic ring of $F346^{7.35}$ results in a

Molecular Pharmacology Fast Forward. Published on April 19, 2010 as DOI: 10.1124/mol.110.064584
This article has not been copyedited and formatted. The final version may differ from this version.

statistically significant gain of binding affinity. EMPA is not affected by this mutation since it does not reach close enough to this sidechain in order to form a direct interaction. Furthermore, the effect of Q134A$^{3.32}$ on almorexant can be explained by a hydrogen bond between Q134$^{3.32}$ and the amide group in this antagonist. EMPA cannot form such an interaction with these residues. It should be noted that the importance of the W214$^{45.54}$ and Y354$^{7.43}$ can not be explained from our docking model. W214$^{5.54}$ is located on the extracellular loop E2 and is, according to our model, far away from the antagonist binding side. Nevertheless, its location at the entrance of the channel leading to the binding cavity might affect the kinetic characteristics of the antagonists by influencing their entry into the binding site.

Fig. 7A shows the docking of almorexant to hOX$_1$, which is essentially the same than its docking to the hOX$_2$ homology model. The only difference between OX$_2$ and OX$_1$ in the closer environment of almorexant is T135A$^{3.33}$. Interestingly, while the T135A$^{3.33}$ mutation in the OX$_2$ receptor did not affect almorexant binding, A127T$^{3.33}$ in OX$_1$ affected almorexant. This cannot be explained from the docking model. However, the introduction of the threonine residue and thus an OH group with its capabilities to form hydrogen bond might result in a change of the local environment that is different from the OX$_2$ receptor due to additional differences between OX$_2$ and OX$_1$ further away from almorexant. Thus, it might be an indirect effect on almorexant binding and functionality. Finally, **Fig. 7B** shows a possible docking mode of SB-674042 to hOX$_1$. It is essentially located in the same region as almorexant. Since it does not come so close to the extracellular loop E2 than almorexant, it is however not affected by the D203A$^{45.51}$ mutation.

Molecular Pharmacology Fast Forward. Published on April 19, 2010 as DOI: 10.1124/mol.110.064584
This article has not been copyedited and formatted. The final version may differ from this version.

Discussion

Here, we have determined the likely binding pockets of OX antagonists, almorexant, EMPA, and SB-674042 using hβ2AR-based modeling of OX-7TMDs and site-directed mutagenesis. Based on the proposed docking mode of almorexant onto the OX_1- and OX_2-7TMD binding cavities, twenty-nine point-mutations (eighteen in OX_2 and eleven in OX_1) located in the TM2, -3, -5, -6, -7, and ECL2b regions were selected as candidates for mutational studies. These mutated hOX_1 and hOX_2 made also possible to probe the orexin-A-binding pockets of OX_1 and OX_2 on the basis of orexin-A-evoked $[Ca^{2+}]_i$ response in the HEK293 cells transiently expressing the mutated receptors.

Binding Site of orexin-A in OX_1 and OX_2. The conserved residues OX_1 $D203^{45.51}$ ($D211^{45.51}$ in OX_2), $W206^{45.54}$ ($W214^{45.54}$ in OX_2), $Y215^{5.38}$ ($Y223^{5.38}$ in OX_2), $F219^{5.42}$ ($F227^{5.42}$ in OX_2), $Y224^{5.47}$ ($Y232^{5.47}$ in OX_2), $Y311^{6.48}$ ($Y317^{6.48}$ in OX_2), and $H344^{7.39}$ ($H350^{6.39}$ in OX_2) were found to be contributing to both orexin-A-binding sites at OX_1 and OX_2, but these residues had yet a more prominent effect on orexin-A's potency at OX_1 than that at OX_2. Orexin-A behaved differently on two residues at TM3 helix positions 3.32 and 3.36 between OX_1 and OX_2. The mutation of OX_2 $Q134^{3.32}$ to alanine caused a 22-fold drop in orexin-A potency at OX_2, whereas the mutation of corresponding residue in OX_1, $Q126A^{3.32}$, had no effect on orexin-A's potency. Conversely, the mutation OX_1 $V130A^{3.36}$ led to a decrease of 31-fold in orexin-A's potency at OX_1, without having any effect on the corresponding residue $V138^{3.36}$ in OX_2. Therefore, the residues OX_1 $V130^{3.36}$ and OX_2 $Q134^{3.32}$ might contribute to the selectivity of orexin-A–OX_1 and –OX_2 binding pockets, respectively. For orexin-A, the conformation and residues required for a high activity at the OX_1 and OX_2 receptors have been extensively characterized. These studies demonstrated that alanine replacement of the same amino acids of orexin-A produced a more prominent reduction in the potency for the OX_1 than that for the OX_2 even though the determinants

Molecular Pharmacology Fast Forward. Published on April 19, 2010 as DOI: 10.1124/mol.110.064584
This article has not been copyedited and formatted. The final version may differ from this version.

required from orexin-A for activation of the receptor was similar between OX_1 and OX_2 (Ammoun et al., 2003; Lang et al., 2004). Interestingly, the reported observations that OX_1 was in general more sensitive to amino acid replacements in orexin-A than OX_2 are in good agreement with our mutational studies of OX_1 and OX_2.

Binding Site of OX antagonists in OX_1 and OX_2. Among eighteen point-mutations that are located in TM2, -3, -5, -6, -7 and ECL2b of hOX_2, we observed that the W214A$^{45.54}$, Y223A$^{5.38}$, F227A$^{5.42}$, Y317A$^{6.48}$ and H350A$^{7.39}$ mutations resulted in complete loss of the [^{3}H]EMPA and [^{3}H]almorexant binding affinities and also blocked the inhibition by both antagonists of orexin-A-evoked $[Ca^{2+}]_i$ response. However, the conversion of Y317$^{6.48}$ to a phenylalanine had no significant effect on almorexant's binding, but a small significant effect on EMPA's binding affinity. This may indicate that the forces involved in the interaction between Y317$^{6.48}$ and almorexant might be via hydrophobic C-H/π interactions. The mutation Y232A$^{5.47}$ led to the complete loss of [^{3}H]EMPA binding affinity and a 37-fold decrease in EMPA's potency, had yet only a moderate effect on [^{3}H]almorexant binding affinity and potency. Notably, three mutations T135A$^{3.33}$, I320A$^{6.51}$, Y354A$^{7.43}$ behaved differently between interacting modes of two antagonists in OX_2, having a detrimental effect on the affinity and potency of EMPA, while almorexant's affinity and potency remained unaffected. Two mutations, T111A$^{2.61}$ and D211A$^{45.51}$, also affected only moderately the binding of EMPA, but not that of almorexant. Of interest is the conserved residue OX_2 V138$^{3.36}$ (V130$^{3.36}$ in OX_1): mutation of this residue affected the binding affinity and functional potency of EMPA (by 15- and 91-fold decrease, respectively), but had no effect on almorexant's binding in OX_1 and OX_2, or SB-674042's binding in OX_1. The V138$^{3.36}$ could be contributing specifically to binding selectivity of EMPA for OX_2. Therefore, it is concluded that the residues T135$^{3.33}$ and V138$^{3.36}$ represent the minimal structural motif responsible for the high selectivity of OX_2 for EMPA. Indeed, in our model, only EMPA's

Molecular Pharmacology Fast Forward. Published on April 19, 2010 as DOI: 10.1124/mol.110.064584
This article has not been copyedited and formatted. The final version may differ from this version.

para-methoxy substituted pyridyl group can reach deep in the subpocket formed by residues T135$^{3.33}$, V138$^{3.36}$ and Y317$^{6.48}$ and additionally, its pyridyl ring can form a H-bond with the hydroxyl group of T135$^{3.33}$ located in close proximity (**Fig. 6B**).

Among the eleven point-mutations that are located in TM3, -5, -6, -7 and ECL2b of hOX$_1$, the mutations Q126A$^{3.32}$, A127T$^{3.33}$, W206A$^{45.54}$, Y215A$^{5.38}$, F219A$^{5.42}$ and H344A$^{7.39}$ abolished the binding affinity and functional potency of both almorexant and SB-674042, yet with a more dramatic effect on almorexant than on SB-674042. The conserved residues D203$^{45.51}$, Y224$^{5.47}$, Y311$^{6.48}$ and Y348$^{7.43}$ of OX$_1$ had completely different behavior between two antagonists: their mutations had detrimental effects on almorexant's binding and function, but had no or small effects on SB-674042. The residue at position 3.33 is of special interest, because it is a non-conservative residue between OX$_1$ (A127$^{3.33}$) and OX$_2$ (T135$^{3.33}$). Conversion of A127$^{3.33}$ to threonine affected dramatically SB-674042 and almorexants' binding affinities and functions at OX$_1$; conversely, conversion of OX$_2$ T135$^{3.33}$ to alanine was detrimental only on EMPA's binding affinity and potency. Hence, the position 3.33 of orexin receptors was identified as a critical position that must be involved in subtype selectivity and also in differentiating two different antagonists for the same receptor, as observed for EMPA and almorexant at OX$_2$.

Comparison of the ligand-binding site in OX$_1$ and OX$_2$ to other class A GPCRs. In Table 5, we have summarized our mutational studies of OX antagonists and compared the critical residues contributing to the ligand-binding sites of OX$_1$ and OX$_2$ with those of rhodopsin (Palczewski et al., 2000; Teller et al., 2001), hβ_2AR (Cherezov et al., 2007; Rosenbaum et al., 2007) and hA$_{2A}$ (Jaakola et al., 2008). The ligand-binding pockets of OX$_1$ and OX$_2$ are very similar, and both offer numerous hydrophobic interactions, predominantly aromatic. Besides, the local conformation of positions 3.32, 3.33 and 3.36 in TM3 and 45.51 in ECL2b might provide the structural basis for pharmacologic selectivity between OX$_1$ and

Molecular Pharmacology Fast Forward. Published on April 19, 2010 as DOI: 10.1124/mol.110.064584
This article has not been copyedited and formatted. The final version may differ from this version.

OX_2. It is interesting to note that among seven critical residues that are shared between orexin-A–OX_1 and –OX_2 binding sites, five residues $D^{45.51}$, $W^{45.54}$, $Y^{5.38}$, $F^{5.42}$ and $H^{7.39}$ are located on the ECL2b and in the top of TM domains at the interface to the main binding crevice, thereby suggesting superficial OX receptor interactions of orexin-A. Similar observation has been reported for other large peptides, such as chemokine receptor interaction with chemokine (Schwarz and Wells, 2002). High resolution β2AR X-ray structure has revealed that the main ligand-binding pocket is a funnel with a partial lid, and that ECL-2b region (highly variable region between the receptors) is an important 7TM structural element forming the edge of this protein lid. In hβ2AR, the formation of a salt bridge between $D192^{45.51}$ on ECL2b and $K305^{7.32}$ on ECL3 at the extracellular end of TM7 is the major structural feature that blocks access to the ligand binding site. Furthermore, an interaction between $F193^{45.53}$ on ECL2b and carazolol was also observed in hβ2AR X-ray structure (Ahuja and Smith, 2009; Cherezov et al., 2007; Rosenbaum et al., 2007). In analogy, OX_1 $D203^{45.51}$ ($D211^{45.51}$ in OX_2) on ECL2b was found to be crucial for orexin-A–OX_1 and –OX_2, EMPA–OX_2 and almorexant–OX_1 binding sites. The OX_1 $W206^{45.54}$ ($W214^{45.54}$ in OX_2), another residue located on ECL2b was also important for OX ligand-binding pocket. Hence, OX receptors might operate with a similar mechanism of activation as β_2AR.

We observed that six OX residues, $W^{45.54}$, $Y^{5.38}$, $F^{5.42}$, $Y^{5.47}$, $Y^{6.48}$ and $H^{7.39}$, are important contributors to the orexin-A–OX_1 and –OX_2, EMPA–OX_2 and almorexant–OX_1 and –OX_2 binding pockets. We speculate that these aromatic residues are involved in a tight network of interhelical aromatic/hydrophobic interactions, which maintains the OX receptors in a constrained/inactive conformation. Consequently, the OX antagonist via intramolecular interactions could further reinforce this network, thereby hindering the structural rearrangements necessary for activation. Of note are the important helix positions 5.47 and 6.48 ($Y^{5.47}$ and $Y^{6.48}$ in OX); as a recent report investigating ghrelin receptor, β2AR and NK_1

Molecular Pharmacology Fast Forward. Published on April 19, 2010 as DOI: 10.1124/mol.110.064584
This article has not been copyedited and formatted. The final version may differ from this version.

has demonstrated that two residues $F^{5.47}$ in TM5 and $W^{6.48}$ (key residue of the rotamer toggle switch) in TM6 are located in close proximity at the bottom of the main ligand-binding pocket and an aromatic interaction between two residues could stabilize the active conformation of $W^{6.48}$ (Holst et al., 2009). Interestingly, two critical residues, $F^{5.42}$ and $H^{7.39}$ (in the top of TM5 and TM7), are positioned on opposite extremities of the ligand-binding pocket. In $h\beta_2AR$, the corresponding positions ($S203^{5.42}$ and $N312^{7.39}$) are involved in H-bond interactions with carazolol (Cherezov et al., 2007; Rosenbaum et al., 2007). Moreover, the position 7.39 in chemokine receptors ($E^{7.39}$, a conserved residue among CCRs) provides an important anchor-point for interaction with nonpeptide agonists and antagonists (Jensen et al., 2007; Rosenkilde and Schwartz, 2006). The position 7.39 was also found to be the critical residue in the binding pocket of other peptide receptors including hNK_2 ($F293^{7.39}$), hNK_3 ($F342^{7.39}$), hV_{1a} ($A334^{7.39}$) and hV_{1b} ($M324^{7.39}$) (Derick et al., 2004; Huang et al., 1995; Malherbe et al., 2008). In conclusion, we have demonstrated for the first time the important molecular determinants of ligand-binding site of OX_1 and OX_2.

Acknowledgements

We are grateful to Marie-Laure Heusler and Marie-Thérèse Zenner for their excellent technical assistance.

References

Ahuja S and Smith SO (2009) Multiple switches in G protein-coupled receptor activation. *Trends Pharmacol Sci* **30**:494-502.

Alexander SP, Mathie A and Peters JA (2008) Guide to Receptors and Channels (GRAC), 3rd edition. *Br J Pharmacol* **153**:S1-209.

Ammoun S, Holmqvist T, Shariatmadari R, Oonk HB, Detheux M, Parmentier M, Akerman KE and Kukkonen JP (2003) Distinct recognition of OX1 and OX2 receptors by orexin peptides. *J Pharmacol Exp Ther* **305**:507-514.

Ballesteros JA and Weinstein H (1995) Integrated methods for construction three-dimensional models and computational probing of structure-function relations in G protein-coupled receptors. *Methods Neurosci* **25**:366-428.

Boss C, Brisbare-Roch C and Jenck F (2009) Biomedical application of orexin/hypocretin receptor ligands in neuroscience. *J Med Chem* **52**:891-903.

Brisbare-Roch C, Dingemanse J, Koberstein R, Hoever P, Aissaoui H, Flores S, Mueller C, Nayler O, van Gerven J, de Haas SL, Hess P, Qiu C, Buchmann S, Scherz M, Weller T, Fischli W, Clozel M and Jenck F (2007) Promotion of sleep by targeting the orexin system in rats, dogs and humans. *Nat Med* **13**:150-155.

Cherezov V, Rosenbaum DM, Hanson MA, Rasmussen SG, Thian FS, Kobilka TS, Choi HJ, Kuhn P, Weis WI, Kobilka BK and Stevens RC (2007) High-resolution crystal structure of an engineered human beta2-adrenergic G protein-coupled receptor. *Science* **318**:1258-1265.

Darker JG, Porter RA, Eggleston DS, Smart D, Brough SJ, Sabido-David C and Jerman JC (2001) Structure-activity analysis of truncated orexin-A analogues at the orexin-1 receptor. *Bioorg Med Chem Lett* **11**:737-740.

de Lecea L, Kilduff TS, Peyron C, Gao X, Foye PE, Danielson PE, Fukuhara C, Battenberg EL, Gautvik VT, Bartlett FS, 2nd, Frankel WN, van den Pol AN, Bloom FE, Gautvik KM and Sutcliffe JG (1998) The hypocretins: hypothalamus-specific peptides with neuroexcitatory activity. *Proc Natl Acad Sci U S A* **95**:322-327.

Derick S, Pena A, Durroux T, Wagnon J, Serradeil-Le Gal C, Hibert M, Rognan D and Guillon G (2004) Key amino acids located within the transmembrane domains 5 and 7 account for the pharmacological specificity of the human V1b vasopressin receptor. *Mol Endocrinol* **18**:2777-2789.

Holst B, Nygaard R, Valentin-Hansen L, Bach A, Engelstoft MS, Petersen PS, Frimurer TM and Schwartz TW (2009) A Conserved aromatic lock for the Tryptophan Rotameric Switch in TM-VI of 7TM receptors. *J Biol Chem* **285**:3973-3985.

Huang RR, Vicario PP, Strader CD and Fong TM (1995) Identification of residues involved in ligand binding to the neurokinin-2 receptor. *Biochemistry* **34**:10048-10055.

Jaakola VP, Griffith MT, Hanson MA, Cherezov V, Chien EY, Lane JR, Ijzerman AP and Stevens RC (2008) The 2.6 angstrom crystal structure of a human A2A adenosine receptor bound to an antagonist. *Science* **322**:1211-1217.

Jensen PC, Nygaard R, Thiele S, Elder A, Zhu G, Kolbeck R, Ghosh S, Schwartz TW and Rosenkilde MM (2007) Molecular interaction of a potent nonpeptide agonist with the chemokine receptor CCR8. *Mol Pharmacol* **72**:327-340.

Kilduff TS and Peyron C (2000) The hypocretin/orexin ligand-receptor system: Implications for sleep and sleep disorders. *Trends Neurosci* **23**:359-365.

Lang M, Bufe B, De Pol S, Reiser O, Meyerhof W and Beck-Sickinger AG (2006) Structural properties of orexins for activation of their receptors. *J Pept Sci* **12**:258-266.

Lang M, Soll RM, Durrenberger F, Dautzenberg FM and Beck-Sickinger AG (2004) Structure-activity studies of orexin A and orexin B at the human orexin 1 and orexin 2

receptors led to orexin 2 receptor selective and orexin 1 receptor preferring ligands. *J Med Chem* **47**:1153-1160.

Langmead CJ, Jerman JC, Brough SJ, Scott C, Porter RA and Herdon HJ (2004) Characterisation of the binding of [3H]-SB-674042, a novel nonpeptide antagonist, to the human orexin-1 receptor. *Br J Pharmacol* **141**:340-346.

Malherbe P, Bissantz C, Marcuz A, Kratzeisen C, Zenner MT, Wettstein JG, Ratni H, Riemer C and Spooren W (2008) Me-talnetant and osanetant interact within overlapping but not identical binding pockets in the human tachykinin neurokinin 3 receptor transmembrane domains. *Mol Pharmacol* **73**:1736-1750.

Malherbe P, Borroni E, Gobbi L, Knust H, Nettekoven M, Pinard E, Roche O, Rogers-Evans M, Wettstein J and Moreau JL (2009a) Biochemical and behavioural characterization of EMPA, a novel high-affinity, selective antagonist for the OX2 receptor. *Br J Pharmacol* **156**:1326-1341.

Malherbe P, Borroni E, Pinard E, Wettstein JG and Knoflach F (2009b) Biochemical and electrophysiological characterization of almorexant, a dual OX1/OX2 antagonist: comparison with selective OX1 and OX2 antagonists. *Mol Pharmacol* **76**:618-631.

Marcus JN, Aschkenasi CJ, Lee CE, Chemelli RM, Saper CB, Yanagisawa M and Elmquist JK (2001) Differential expression of orexin receptors 1 and 2 in the rat brain. *J Comp Neurol* **435**:6-25.

Nambu T, Sakurai T, Mizukami K, Hosoya Y, Yanagisawa M and Goto K (1999) Distribution of orexin neurons in the adult rat brain. *Brain Res* **827**:243-260.

Neubauer DN (2010) Almorexant, a dual orexin receptor antagonist for the treatment of insomnia. *Curr Opin Investig Drugs* **11**:101-110.

Nishino S (2007) The hypocretin/orexin receptor: therapeutic prospective in sleep disorders. *Expert Opin Investig Drugs* **16**:1785-1797.

Nygaard R, Frimurer TM, Holst B, Rosenkilde MM and Schwartz TW (2009) Ligand binding and micro-switches in 7TM receptor structures. *Trends Pharmacol Sci* **30**:249-259.

Ohno K and Sakurai T (2008) Orexin neuronal circuitry: role in the regulation of sleep and wakefulness. *Front Neuroendocrinol* **29**:70-87.

Palczewski K, Kumasaka T, Hori T, Behnke CA, Motoshima H, Fox BA, Le Trong I, Teller DC, Okada T, Stenkamp RE, Yamamoto M and Miyano M (2000) Crystal structure of rhodopsin: A G protein-coupled receptor. *Science* **289**:739-745.

Peyron C, Tighe DK, van den Pol AN, de Lecea L, Heller HC, Sutcliffe JG and Kilduff TS (1998) Neurons containing hypocretin (orexin) project to multiple neuronal systems. *J Neurosci* **18**:9996-10015.

Roecker AJ and Coleman PJ (2008) Orexin receptor antagonists: medicinal chemistry and therapeutic potential. *Curr Top Med Chem* **8**:977-987.

Rosenbaum DM, Cherezov V, Hanson MA, Rasmussen SG, Thian FS, Kobilka TS, Choi HJ, Yao XJ, Weis WI, Stevens RC and Kobilka BK (2007) GPCR engineering yields high-resolution structural insights into beta2-adrenergic receptor function. *Science* **318**:1266-1273.

Rosenkilde MM and Schwartz TW (2006) GluVII:06--a highly conserved and selective anchor point for non-peptide ligands in chemokine receptors. *Curr Top Med Chem* **6**:1319-1333.

Sakurai T, Amemiya A, Ishii M, Matsuzaki I, Chemelli RM, Tanaka H, Williams SC, Richardson JA, Kozlowski GP, Wilson S, Arch JR, Buckingham RE, Haynes AC, Carr SA, Annan RS, McNulty DE, Liu WS, Terrett JA, Elshourbagy NA, Bergsma DJ and Yanagisawa M (1998) Orexins and orexin receptors: a family of hypothalamic neuropeptides and G protein-coupled receptors that regulate feeding behavior. *Cell* **92**:573-585.

Schwarz MK and Wells TN (2002) New therapeutics that modulate chemokine networks. *Nat Rev Drug Discov* **1**:347–358.

Takai T, Takaya T, Nakano M, Akutsu H, Nakagawa A, Aimoto S, Nagai K and Ikegami T (2006) Orexin-A is composed of a highly conserved C-terminal and a specific, hydrophilic N-terminal region, revealing the structural basis of specific recognition by the orexin-1 receptor. *J Pept Sci* **12**:443-454.

Tang J, Chen J, Ramanjaneya M, Punn A, Conner AC and Randeva HS (2008) The signalling profile of recombinant human orexin-2 receptor. *Cell Signal* **20**:1651-1661.

Teller DC, Okada T, Behnke CA, Palczewski K and Stenkamp RE (2001) Advances in determination of a high-resolution three-dimensional structure of rhodopsin, a model of G-protein-coupled receptors (GPCRs). *Biochemistry* **40**:7761-7772.

Trivedi P, Yu H, MacNeil DJ, Van der Ploeg LH and Guan XM (1998) Distribution of orexin receptor mRNA in the rat brain. *FEBS Lett* **438**:71-75.

Molecular Pharmacology Fast Forward. Published on April 19, 2010 as DOI: 10.1124/mol.110.064584
This article has not been copyedited and formatted. The final version may differ from this version.

Legends for Figures

Fig. 1: (A) Chemical structures of the selective OX_1, OX_2 and dual OX_1/OX_2 antagonists. T, tritium. (B) The amino acid sequences of orexin-A and -B. Orexin-A have a pyroglutamate (2-pyrrolidone-5-carboxylic acid) at the first N-terminal residue site, which is indicated by U. The C-terminal of both orexins *(*–NH2*)* are amidated. Two intramolecular disulfide bonds in orexin-A formed between C6 and C12, and between C7 and C14 are shown as lines. The residues, identical in both orexins, are highlighted in gray.

Fig. 2: Amino acid sequence alignment of the TM1–Helix 8 region of the hOX_1 with the hOX_2 using pairwise global alignment (Needleman-Wunsch algorithm). The numbers on the right refer to the amino acids of hOX_1 and hOX_2 receptors. Vertical lines indicate identical residues and colons indicate conservative replacement of residues (chemically homologous residues) between hOX_1 and OX_2. The transmembrane (TM) domains are boxed. The conserved residue in each TM which is assigned to 50 according to Ballesteros Weinstein numbering scheme is shown by black arrows. The critical residues (indicating by Ballesteros Weinstein numbering scheme of the amino acids) in the binding pocket of orexin receptor antagonists (almorexant, EMPA, SB-674042) are shown by red boldface type and red short arrows. Three conserved motifs in TM3 (DRY), TM6 (CWxP) and TM7 (NPxxY) that is believed to function as a micro-switches (Nygaard et al., 2009), are shown in blue boldface type and underlined. ECL, extracellular loop; ICL, intracellular loop.

Fig. 3: A, Alignment of the amino acids forming the binding site of OX_1 and OX_2 relative to bovine rhodopsin (P02699), human β_2-adrenergic (P07750) and human A_{2A} (P29274) receptors. Ballesteros Weinstein numbering scheme of the amino acids (indicated above the TMs in the bottom row) are given to facilitate the comparison with other GPCR's (see

Materials and Mehods). The numbers above the OX1R_HUMAN and OX2R_HUMAN receptors give the sequence number of the positions of the mutations carried out in this study. The residue at helix position 3.33, which is different between OX_1 and OX_2 binding pockets are boxed and yellow high-lighted.

Fig. 4: Effects of orexin antagonists on orexin-A-evoked $[Ca^{2+}]_i$ in WT and mutated hOX_2 receptors. Concentration-dependent inhibition of OX-A (EC_{80} value) stimulated increases in $[Ca^{2+}]_i$ by EMPA (panels A, C and E) and almorexant (panels B, D and F) as assayed using the Ca^{2+}-sensitive dye, Flou-4 and a Fluorometric Imaging Plate Reader in HEK293 transiently transfected with the hOX_2 WT and mutated receptors. Responses are normalized to the first control response. Each curve represents the mean of six dose-response measurements (each performed in duplicate) from three independent transfections.

Fig. 5: Effects of orexin antagonists on orexin-A-evoked $[Ca^{2+}]_i$ in WT and mutated hOX_1 receptors. Concentration-dependent inhibition of orexin-A (EC_{80} value) stimulated increases in $[Ca^{2+}]_i$ by SB-674042 (panels A and C) and almorexant (panels B and D) as assayed using the Ca^{2+}-sensitive dye, Flou-4 and a Fluorometric Imaging Plate Reader in HEK293 transiently transfected with the hOX_1 WT and mutated receptors. Responses are normalized to the first control response. Each curve represents the mean of 6 dose-response measurements (each performed in duplicate) from three independent transfections.

Fig. 6: (A) and (B): Predicted docking poses of almorexant (A) and EMPA (B) in the OX_2 binding site. Shown are the residues that were found to be important according to our mutational studies. Ligand carbon atoms are shown in magenta, protein carbon atoms are shown in green. Nitrogen atoms are shown in blue, oxygen in red, sulfur atoms in yellow and

Molecular Pharmacology Fast Forward. Published on April 19, 2010 as DOI: 10.1124/mol.110.064584
This article has not been copyedited and formatted. The final version may differ from this version.

fluorine atoms in green. The possible hydrogen bond interactions between $Q134^{3.32}$ with almorexant in A and $T135^{3.33}$ with EMPA in B are visualized by red dotted lines. (C): Predicted docking poses of both almorexant (cyan) and EMPA (magenta) in the OX_2 binding site. Shown in grey are protein carbon atoms of residues that were important for almorexant and EMPA according to our mutational studies. Shown in cyan are protein carbon atoms of residues that were important for only almorexant according to our mutational studies. Shown in magenta are protein carbon atoms of residues that were important for only EMPA according to our mutational studies. Nitrogen atoms are shown in blue, oxygen in red, sulfur atoms in yellow and fluorine atoms in green.

Fig. 7: Predicted docking poses of almorexant (A) and SB674042 (B) in the OX_1 binding site. Shown are the residues that were found to be important according to our mutational studies. Ligand carbon atoms are shown in magenta, protein carbon atoms are shown in green. Nitrogen atoms are shown in blue, oxygen atoms in red and fluorine atoms in green.

Molecular Pharmacology Fast Forward. Published on April 19, 2010 as DOI: 10.1124/mol.110.064584
This article has not been copyedited and formatted. The final version may differ from this version.

Tables

Table 1. The effect of mutations on OX_2-mediated of orexin-A-induced $[Ca^{2+}]_i$ response. EC_{50}, Hill slope (n_H), and relative efficacy (E_{max}) values for the orexin-A-induced $[Ca^{2+}]_i$ response in the HEK293 cells transiently transfected with the WT and mutated hOX_2 receptors. The data is mean ± S.E. of eight concentration-response measurements (each performed in duplicate) from four independent transfections. The mutations that affected the potency of orexin-A in comparison to WT are shown in boldface type.

hOX_2	7TM position	orexin-A			
		EC_{50} nM	EC_{50} (mut)/ EC_{50} (WT)	Hill	E_{max} relative
WT		0.6 ± 0.1		0.5 ± 0.0	100
T111A	2.61	151.0 ± 22.2	**243.5**	0.7 ± 0.0	114.4 ± 13.0
Q134A	3.32	13.8 ± 2.1	**22.3**	1.4 ± 0.1	62.3 ± 1.1
T135A	3.33	0.5 ± 0.1	0.8	0.6 ± 0.1	109.3 ± 11.2
V138A	3.36	2.8 ± 0.4	4.4	0.7 ± 0.0	92.1 ± 10.0
S139A	3.37	1.5 ± 0.3	2.5	0.6 ± 0.0	86.1 ± 8.6
D211A	45.51	258.0 ± 57.2	**416.1**	0.8 ± 0.1	126.4 ± 16.4
W214A	45.54	38.7 ± 12.2	**62.4**	0.7 ± 0.1	71.3 ± 7.4
Y223A	5.38	114.0 ± 14.1	**183.9**	1.0 ± 0.1	61.2 ± 1.2
F227A	5.42	149.0 ± 34.8	**240.3**	1.1 ± 0.1	64.3 ± 6.3
F228A	5.43	1.8 ± 0.7	3.0	0.7 ± 0.1	76.2 ± 2.1
Y232A	5.47	17.6 ± 3.1	**28.4**	1.2 ± 0.1	44.9 ± 4.5
Y317A	6.48	11.0 ± 6.1	**17.7**	1.0 ± 0.1	49.6 ± 6.7
Y317F	6.48	0.8 ± 0.3	1.3	0.6 ± 0.1	72.3 ± 9.7
I320A	6.51	0.6 ± 0.2	0.9	0.6 ± 0.0	97.0 ± 5.4
F346A	7.35	33.8 ± 8.8	**54.5**	1.1 ± 0.2	60.7 ± 13.2
H350A	7.39	30.7 ± 5.2	**49.5**	1.1 ± 0.2	63.0 ± 10.7
V353A	7.42	1.2 ± 0.5	1.9	0.6 ± 0.1	84 8 ± 14.7
Y354A	7.43	2.3 ± 0.9	3.7	0.7 ± 0.1	66.1 ± 12.0

Molecular Pharmacology Fast Forward. Published on April 19, 2010 as DOI: 10.1124/mol.110.064584
This article has not been copyedited and formatted. The final version may differ from this version.

Table 2. The effect of mutations on OX_1-mediated of orexin-A-induced $[Ca^{2+}]_i$ response.

EC_{50}, Hill slope (n_H), and relative efficacy (E_{max}) values for the orexin-A-induced $[Ca^{2+}]_i$ response in the HEK293 cells transiently transfected with the WT and mutated hOX_1 receptors. The data is mean ± S.E. of eight concentration-response measurements (each performed in duplicate) from four independent transfections. The mutations that affected the potency and relative efficacy of orexin-A in comparison to WT are shown in boldface type.

hOX_1	7TM position	orexin-A			
		EC_{50} nM	EC_{50} (mut)/ EC_{50} (WT)	Hill	E_{max} relative
WT		0.9 ± 0.2		0.7 ± 0.1	100
Q126A	3.32	2.2 ± 0.2	2.4	0.7 ± 0.1	59.1 ± 10.1
A127T	3.33	1.6 ± 0.4	1.8	0.8 ± 0.0	97.9 ± 32.9
V130A	3.36	27.5 ± 2.5	**30.6**	0.7 ± 0.1	98.9 ± 31.4
D203A	45.51	367.4 ± 75.0	**408.2**	0.8 ± 0.1	155.2 ± 53.1
W206A	45.54	376.0 ± 102.0	**417.8**	0.8 ± 0.2	45.0 ± 8.0
Y215A	5.38	367.0 ± 95.0	**407.8**	0.6 ± 0.1	65.0 ± 9.0
F219A	5.42	125.6 ± 26.5	**139.6**	0.8 ± 0.1	90.1 ± 48.6
Y224A	5.47	76.0 ± 41.3	**84.4**	0.6 ± 0.1	83.7 ± 40.6
Y311A	6.48	147.5 ± 67.1	**163.9**	0.9 ± 0.1	53.4 ± 12.9
H344A	7.39	217.0 ± 63.9	**241.1**	0.9 ± 0.1	64.5 ± 7.3
Y348A	7.43	7.8 ± 3.0	8.7	0.8 ± 0.0	62.4 ± 18.9

Molecular Pharmacology Fast Forward. Published on April 19, 2010 as DOI: 10.1124/mol.110.064584
This article has not been copyedited and formatted. The final version may differ from this version.

Table 3. Comparison of mutation effects on binding and functional potencies of antagonists at OX_2.

[^{3}H]EMPA and [^{3}H]almorexant binding properties at human wild type and mutated hOX_2 receptors. Saturation binding isotherms of [^{3}H]EMPA and [^{3}H]almorexant were performed on membrane preparations from HEK293 cells transiently transfected with the WT and mutated hOX_2 as described under "Materials and Methods". The K_d and B_{max} values are mean ± S.E., calculated at least from 3-5 independent experiments (each performed in triplicate). Statistical significance was determined using the two-tailed t-test: *P<0.05, **P<0.01, ***P<0.001.
Effects of mutations on inhibition of orexin-A-induced $[Ca^{2+}]_i$ response by EMPA and almorexant. K_b and Hill coefficient (n_H) values for the inhibition by EMPA and almorexant of orexin-A (EC_{80} value)-evoked $[Ca^{2+}]_i$ response in the HEK293 cells transiently transfected with the hOX_2 WT and mutated receptors. Data are means ± S.E. of the six dose-response measurements (each performed in duplicate) from three independent transfections. The mutations that affected the binding and functional potencies of EMPA and almorexant in comparison to the WT are shown in boldface type. N.D.B., no detectable binding due to high nonspecific binding.

hOX_2	Position in the 7TMD	[^{3}H]EMPA binding			EMPA (FLIPR)			[^{3}H]almorexant binding			almorexant (FLIPR)		
		K_d nM	K_d (mut)/ K_d (WT)	B_{max} pmol/mg protein	K_b nM	K_b (mut)/ K_b (WT)	n_H	K_d nM	K_d (mut)/ K_d (WT)	B_{max} pmol/mg protein	K_b nM	K_b (mut)/ K_b (WT)	n_H
WT		1.1 ± 0.0		24.8 ± 0.2	1.1 ± 0.1		0.6 ± 0.0	1.2 ± 0.0		23.1 ± 0.6	2.4 ± 0.1		1.8 ± 0.1
T111A	2.61	8.1 ± 1.9	**7.4***	20.8 ± 3.4	56.2 ± 8.5	**51.1**	0.6 ± 0.1	0.8 ± 0.2	0.7	18.3 ± 2.9	3.4 ± 0.4	1.4	1.1 ± 0.1
Q134A	3.32	1.9 ± 0.3	1.7	4.1 ± 0.2	2.5 ± 0.3	2.3	0.9 ± 0.0	12.8 ± 5.5	**10.7***	18.0 ± 6.1	4.4 ± 0.5	1.8	1.7 ± 0.3
T135A	3.33	**N.D.B.**			3270.0 ± 97.4	**2972.7**	0.6 ± 0.1	1.0 ± 0.2	0.8	11.9 ± 1.3	7.2 ± 0.1	3.0	2.6 ± 0.2
V138A	3.36	16.4 ± 0.8	**14.9*****	18.1 ± 1.4	100.0 ± 12.6	**90.9**	0.6 ± 0.0	1.6 ± 0.1	1.3	18.4 ± 1.8	3.1 ± 0.8	1.3	2.0 ± 0.1
S139A	3.37	1.8 ± 0.1	1.6	4.0 ± 0.3	2.2 ± 0.4	2.0	0.8 ± 0.0	1.8 ± 1.0	1.5	4.5 ± 1.2	3.6 ± 0.6	1.5	2.1 ± 0.1
D211A	45.51	9.6 ±1.2	**8.7****	11.6 ± 1.0	18.5 ± 2.0	**16.8**	0.7 ± 0.0	0.7 ± 0.2	0.6	9.4 ± 0.9	6.3 ± 0.6	2.6	1.7 ± 0.1
W214A	45.54	**N.D.B.**			**>10,000**			**N.D.B.**			**>10,000**		
Y223A	5.38	**N.D.B.**			372.9 ± 56.0	**339.0**	3.1 ± 0.9	**N.D.B.**			**>10,000**		
F227A	5.42	**N.D.B.**			462.0 ± 13.9	**420.0**	1.4 ± 0.0	**N.D.B.**			481.0 ± 42.1	**200.4**	0.4 ± 0.1
F228A	5.43	3.3 ± 0.9	3.0	10.1 ± 0.8	3.1 ± 0.6	2.8	0.5 ± 0.1	1.1 ± 0.2	0.9	10.0 ± 1.1	2.6 ± 0.3	1.1	1.6 ± 0.2
Y232A	5.47	**N.D.B.**			40.8 ± 6.5	**37.1**	1.0 ± 0.1	**11.6 ± 1.9**	**10.0****	14.6 ± 2.1	18.1 ± 1.6	**7.5**	1.3 ± 0.2
Y317A	6.48	**N.D.B.**			60.0 ± 7.1	**54.5**	1.0 ± 0.1	**N.D.B.**			59.9 ± 5.1	**25.0**	1.2 ± 0.3
Y317F	6.48	6.2 ± 0.9	**3.9****	12.6 ± 2.5	10.4 ± 0.7	**9.5**	1.0 ± 0.1	1.0 ± 0.0	0.8	5.2 ± 0.1	4.0 ± 0.6	1.7	1.8 ± 0.2
I320A	6.51	**N.D.B.**			457.0 ± 20.9	**415.5**	0.7 ± 0.2	0.8 ± 0.2	0.7	11.2 ± 1.3	3.1 ± 0.8	1.3	1.0 ± 0.2
F346A	7.35	1.6 ± 0.1	1.4	11.8 ± 0.3	1.5 ± 0.2	1.4	1.0 ± 0.0	0.4 ± 0.1	**0.3*****	10.6 ± 0.4	1.9 ± 0.3	0.8	1.5 ± 0.4
H350A	7.39	**N.D.B.**			307.0 ± 35.1	**279.1**	1.0 ± 0.2	**N.D.B.**			**226.0 ± 63.2**	**94.2**	0.5 ± 0.1
V353A	7.42	3.1 ± 0.8	2.8	20.8 ± 2.8	4.4 ± 0.2	4.0	0.7 ± 0.1	3.0 ± 1.1	2.5	20.7 ± 3.6	6.2 ± 0.7	2.6	1.1 ± 0.1
Y354A	7.43	**N.D.B.**			403.0 ± 44.8	**366.4**	0.6 ± 0.1	2.6 ± 0.8	2.2	20.1 ± 2.4	4.7 ± 0.3	2.0	0.9 ± 0.0

Molecular Pharmacology Fast Forward. Published on April 19, 2010 as DOI: 10.1124/mol.110.064584
This article has not been copyedited and formatted. The final version may differ from this version.

Table 4. Comparison of mutation effects on binding and functional potencies of antagonists at OX_1.

[^{3}H]SB-674042 and [^{3}H]almorexant binding properties at human wild type and mutated hOX_1receptors. Saturation binding isotherms of [^{3}H]SB-674042 and [^{3}H]almorexant were performed on membrane preparations from HEK293 cells transiently transfected with the WT and mutated hOX_1 as described under "Materials and Methods". The K_d and B_{max} values are mean ± S.E., calculated at least from 3-5 independent experiments (each performed in triplicate). Statistical significance was determined using the two-tailed t-test: *P<0.05, **P<0.01, ***P<0.001.

Effects of mutations on inhibition of orexin-A-induced $[Ca^{2+}]_i$ response by SB-674042 and almorexant. K_b and Hill coefficient (n_H) values for the inhibition by SB-674042 and almorexant of orexin-A (EC_{80})-evoked $[Ca^{2+}]_i$ response in the HEK293 cells transiently transfected with the hOX_1 WT and mutated receptors. Data are means ± S.E. of the 6 dose-response measurements (each performed in duplicate) from three independent transfections. The mutations that affected the binding and functional potencies of [^{3}H]SB-674042 and [^{3}H]almorexant in comparison to the WT are shown in boldface type. N.D.B., no detectable binding due to high nonspecific binding. N. M., not measured.

hOX_1	Position in the 7TMD	[^{3}H]SB-674042 binding			SB-674042 (FLIPR)			[^{3}H]almorexant binding			almorexant (FLIPR)		
		K_d nM	K_d (mut)/ K_d (WT)	B_{max} pmol/mg protein	K_b nM	K_b (mut)/ K_b (WT)	n_H	K_d nM	K_d (mut)/ K_d (WT)	B_{max} pmol/mg protein	K_b nM	K_b (mut)/ K_b (WT)	n_H
WT		1.2 ± 0.0		14 ± 0.4	0.6 ± 0.1		0.5 ± 0.1	2.3 ± 0.3		22.9 ± 2.2	4.8 ± 0.7		0.5 ± 0.0
Q126A	3.32	61.1 ± 6.0	**50.9*** **	10.0 ± 3.8	24.2 ± 8.8	**40.3**	0.9 ± 0.1	**N.D.B.**			**>10,000**		
A127T	3.33	24.2 ± 7.0	**20.2****	15.2 ± 3.0	13.7 ± 1.6	**22.8**	0.5 ± 0.1	**N.D.B.**			**>10,000**		
V130A	3.36	2.5 ± 1.2	2.1	17.6 ± 0.5	0.6 ± 0.3	1.0	0.7 ± 0.0	3.4 ± 1.0	1.5	13.4 ± 2.3	13.1 ± 1.9	2.7	1.1 ± 0.1
D203A	45.51	0.8 ± 0.1	0.7	9.0 ± 0.2	N.M.			**N.D.B.**			N.M.		
W206A	45.54	**N.D.B.**			N.M.			**N.D.B.**			N.M.		
Y215A	5.38	**N.D.B.**			N.M.			**N.D.B.**			N.M.		
F219A	5.42	**N.D.B.**			187.0 ± 77.1	**311.7**	0.5 ± 0.1	**N.D.B.**			921.0 ± 346.5	**191.9**	0.9 ± 0.3
Y224A	5.47	2.2 ± 1.0	1.8	2.2 ± 0.2	0.3 ± 0.0	0.5	0.6 ± 0.0	**N.D.B.**			22.8 ± 3.7	4.8	0.9 ± 0.1
Y311A	6.48	12.9 ± 3.4	**10.8****	2.7 ± 0.3	0.7 ± 0.1	1.2	0.6 ± 0.0	**N.D.B.**			**>10,000**		
H344A	7.39	27.2 ± 4.0	**22.7*****	1.6 ± 0.8	12.5 ± 1.1	**20.8**	0.8 ± 0.0	**N.D.B.**			294.0 ± 97.1	**61.3**	0.3 ± 0.1
Y348A	7.43	11.2 ± 1.0	**9.3*****	3.2 ± 0.1	4.1 ± 0.6	6.8	0.6 ± 0.1	**N.D.B.**			157.0 ± 18.8	**32.7**	0.8 ± 0.1

Molecular Pharmacology Fast Forward. Published on April 19, 2010 as DOI: 10.1124/mol.110.064584
This article has not been copyedited and formatted. The final version may differ from this version.

Table 5. Comparison of ligand-binding pocket of orexin receptor antagonists with those of bovine rhodopsin, hβ$_2$AR and hA$_{2A}$.

The residues located at a distance of 4.5 Å from 11-*cis*-retinal (inverse agonist) in the 3D structure of rhodopsin (2.8 Å, PDB ref code 1F88) (Palczewski et al., 2000; Teller et al., 2001), within 4 Å of the carazolol (partial inverse agonist) in the 2.4 Å resolution crystal structure of human β2-adrenergic receptor (PDB, 2RH1) (Cherezov et al., 2007; Rosenbaum et al., 2007), and within 5 Å of the ZM241385 (subtype-selective antagonist) in the 3D structure of human A_{2A} adenosine receptor (2.6 Å, code 3EML) (Jaakola et al., 2008) are shown for comparison with the critical residues in the binding pocket of orexin receptor antagonists. The generic numbering system proposed by Ballesteros and Weinstein (Ballesteros and Weinstein, 1995) was used to compare residues in the 7TMD of the different GPCR's. WT, the same potency as wild type; (↓), decrease in both binding affinity and potency in comparison with WT; S.E., small but statistically significant decrease in binding affinity; N.A., not available (the mutation was not performed); (↑), increase in binding affinity.

Position in the 7TMD	Opsd_bovin	hβ$_2$AR	hA$_{2A}$	hOX$_1$		hOX$_2$	
	11-*cis*-retinal	carazolol	ZM241385	SB-674042	almorexant	almorexant	EMPA
2.61				N.A.	N.A.	WT	T111A (↓)
3.32	A117	D113		Q126A (↓)	Q126A (↓)	S. E.	WT
3.33	T118	V114	L85	A127T(↓)	A127T (↓)	WT	T135A (↓)
3.36	G121	V117		WT	WT	WT	V138A (↓)
ECL2b (45.51)		D192		WT	D203A (↓)	WT	D211A (↓)
ECL2b (45.54)	Y191			W206A (↓)	W206A (↓)	W214A (↓)	W214A (↓)
5.38	F203	Y199	M177	Y215A (↓)	Y215A (↓)	Y223A (↓)	Y223A (↓)
5.42	M207	S203	N181	F219A (↓)	F219A (↓)	F227A (↓)	F227A (↓)
5.47	F212	F208		WT	Y224A (↓)	Y232A (↓)	Y232A (↓)
6.48	W265	W286	W246	S.E.	Y311A (↓)	Y317A (↓)	Y317A (↓)
6.51	Y268	F289	L249	N.A.	N.A.	WT	I320A (↓)
7.35	M288	Y308	M270	N.A.	N.A.	F346A (↑)	WT
7.39	A292	N312	I274	H344A (↓)	H344A (↓)	H350A (↓)	H350A (↓)
7.43	K296	Y316		S.E.	Y348A (↓)	WT	Y354A (↓)

A

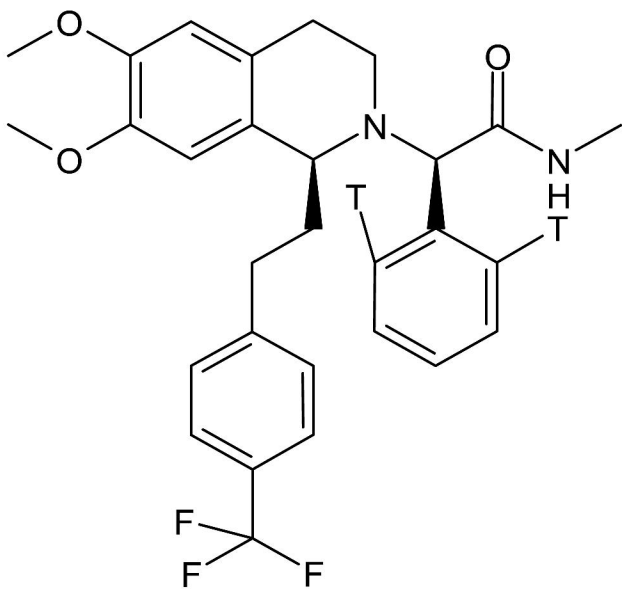

[^{3}H]almorexant
(dual OX_1/OX_2)

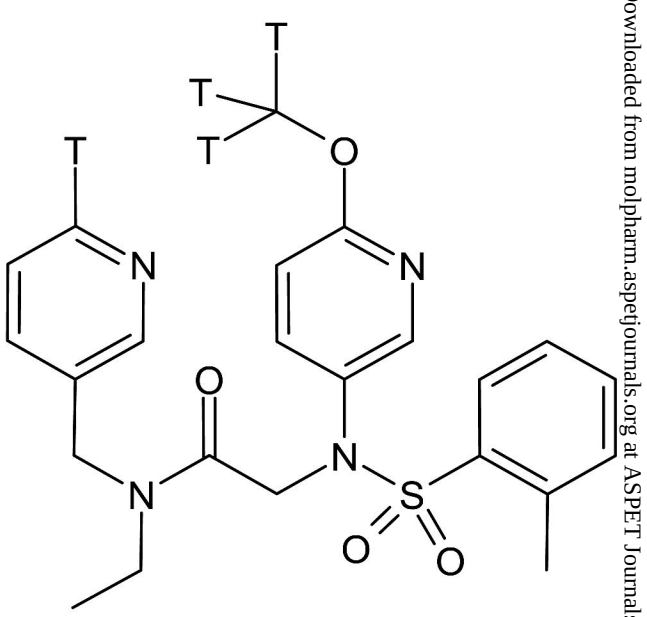

[^{3}H]EMPA
(OX_2-sel)

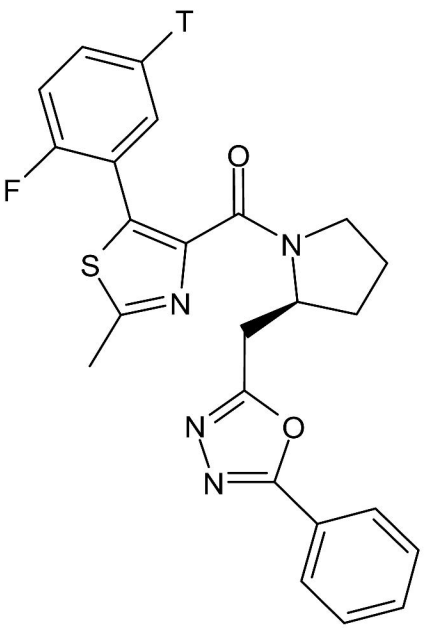

[^{3}H]SB-674042
(OX_1-sel)

B

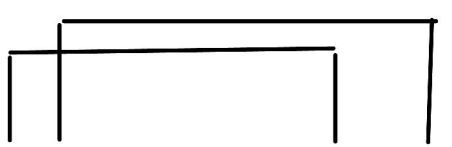

Orexin-A UPLPDCCRQKTCSCRLYELLHGAGNHAAGI LTL-NH2
Orexin-B RSGPPGLQGRLQRLLQASGNHAAGILTM-NH2

Fig. 1

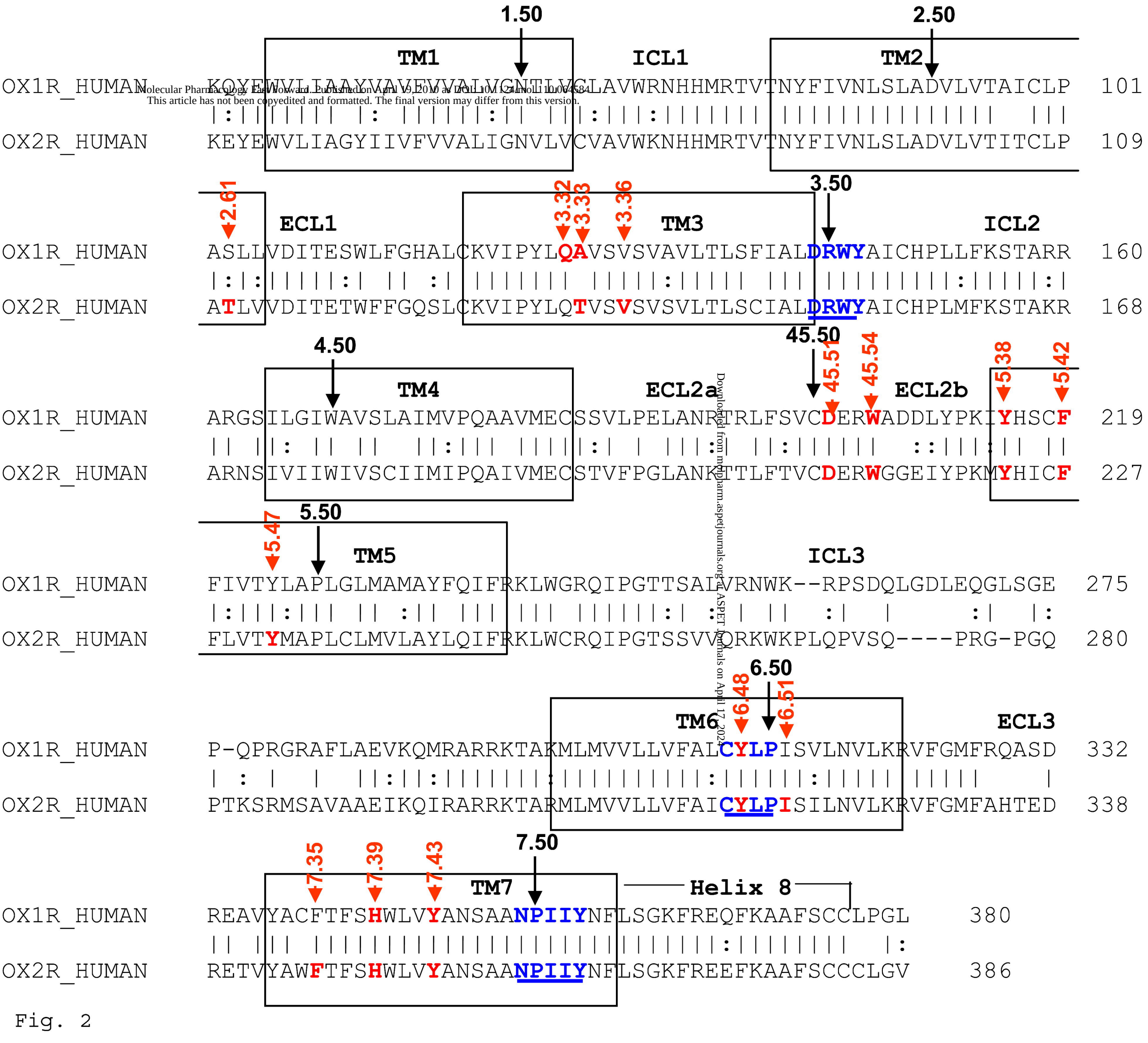

Fig. 2

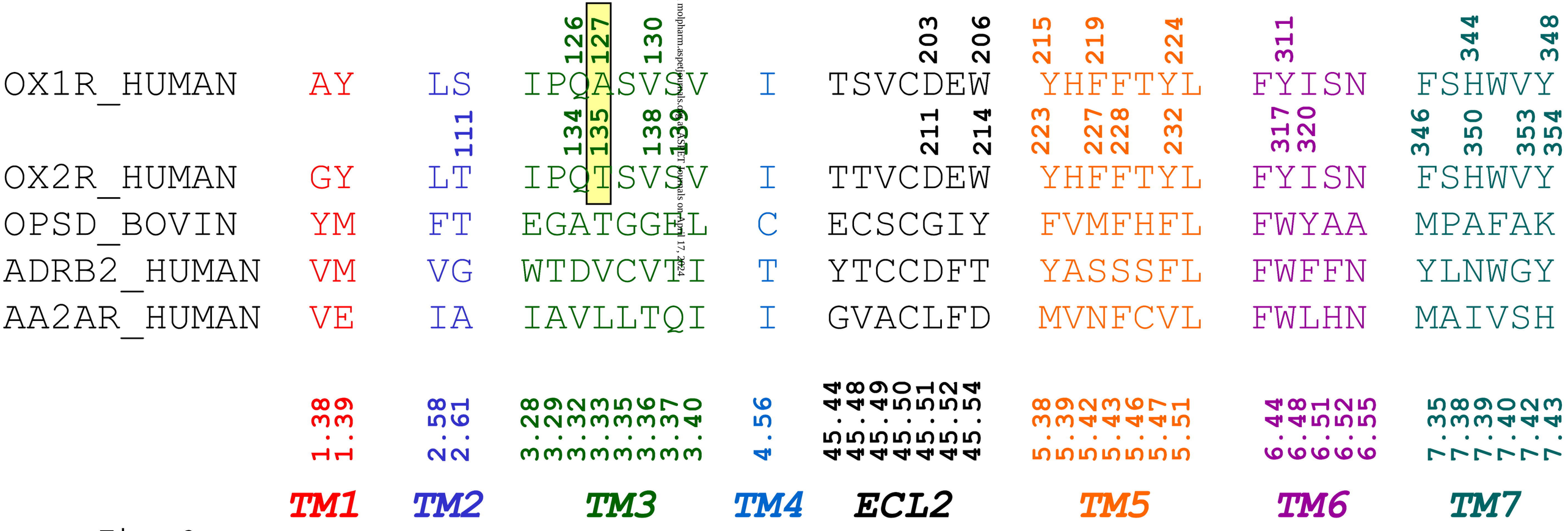

Fig. 3

Fig. 4

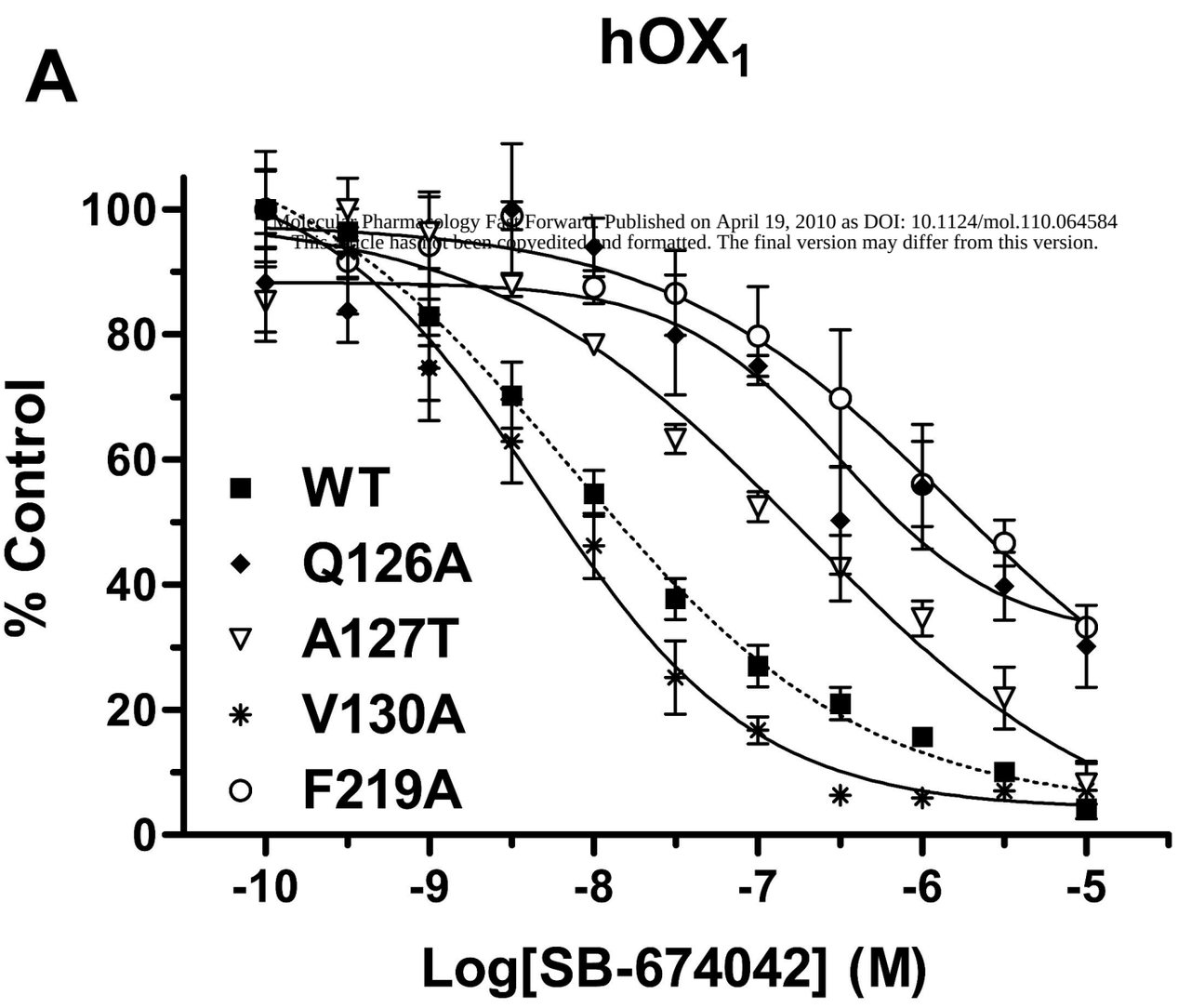

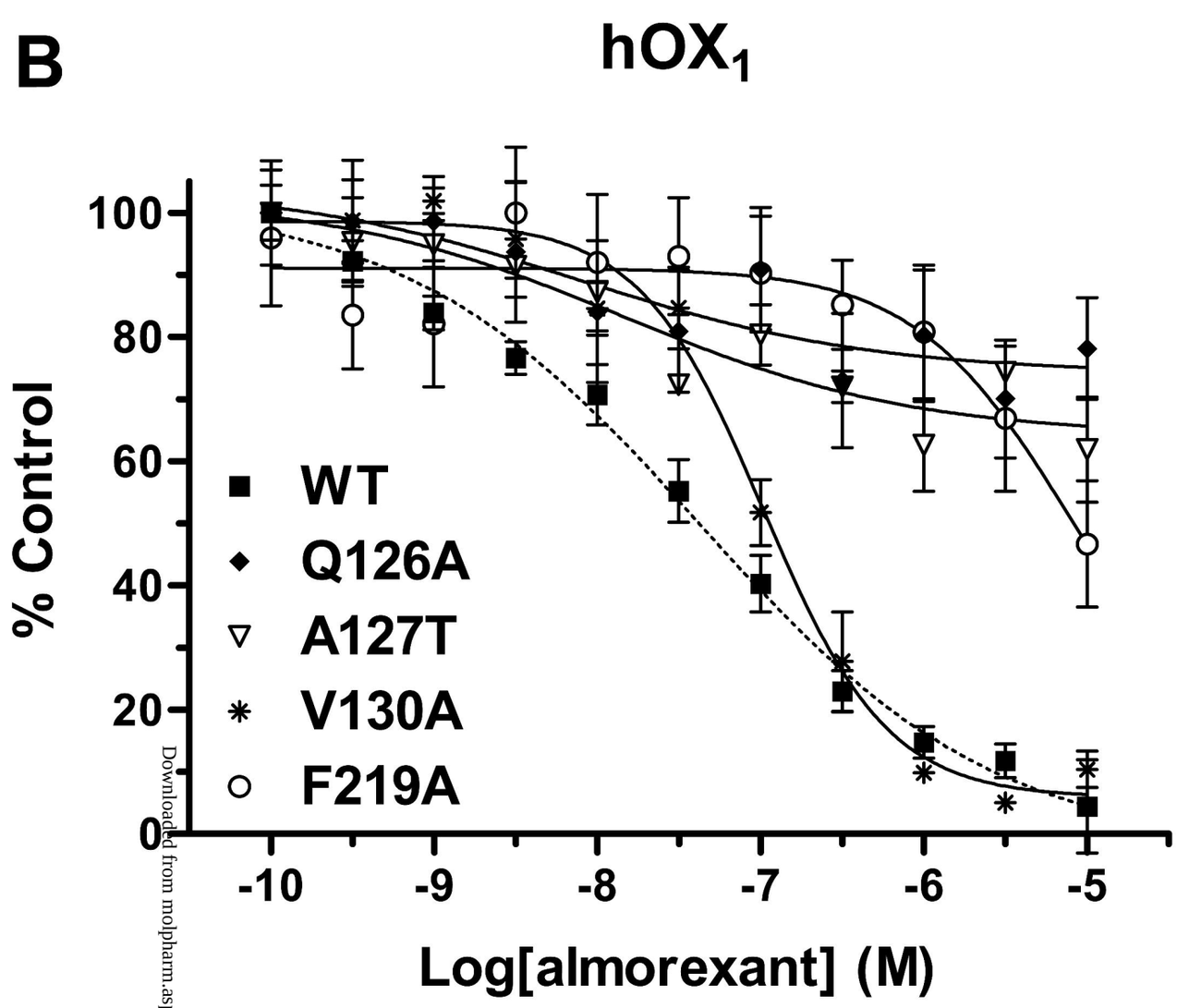

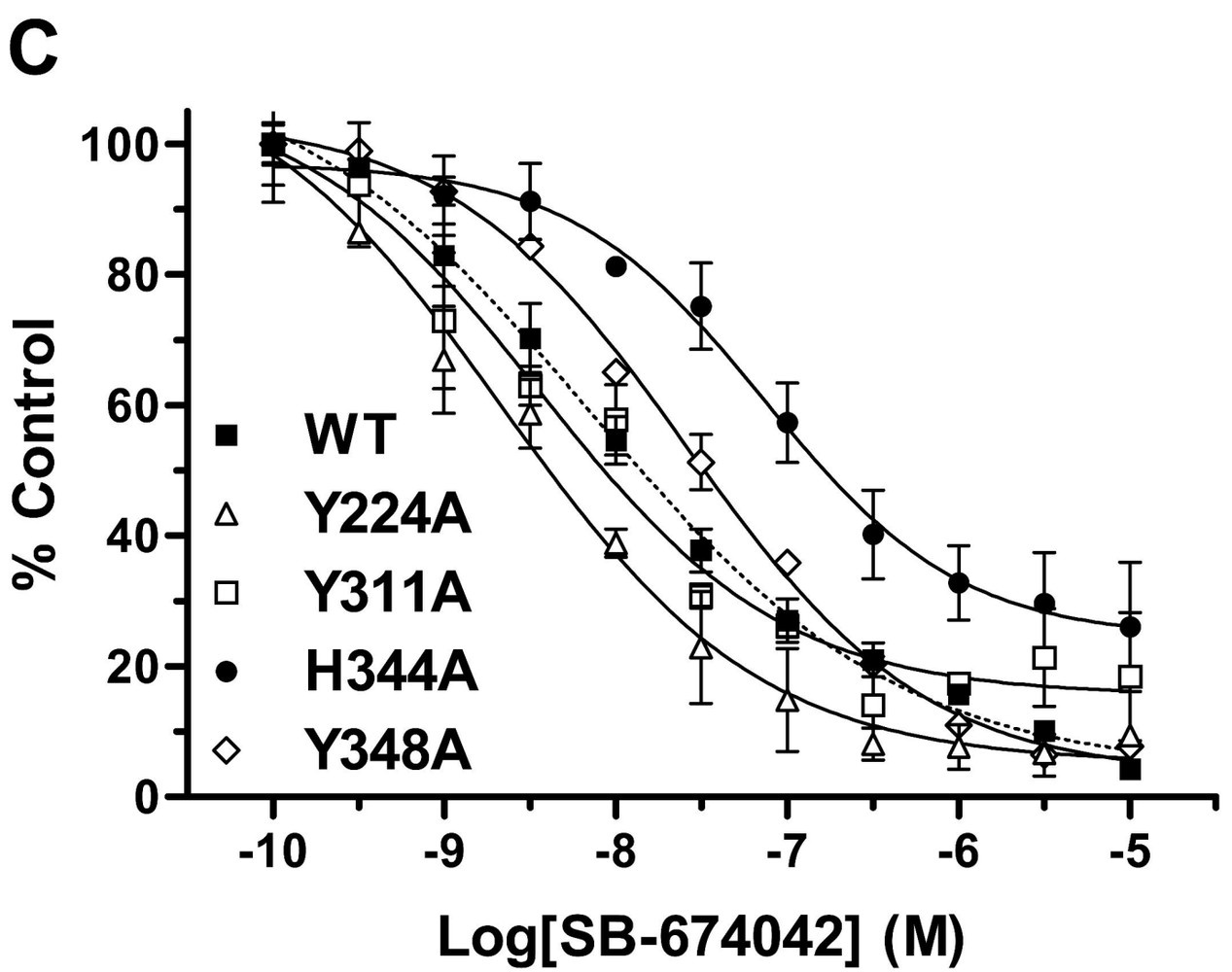

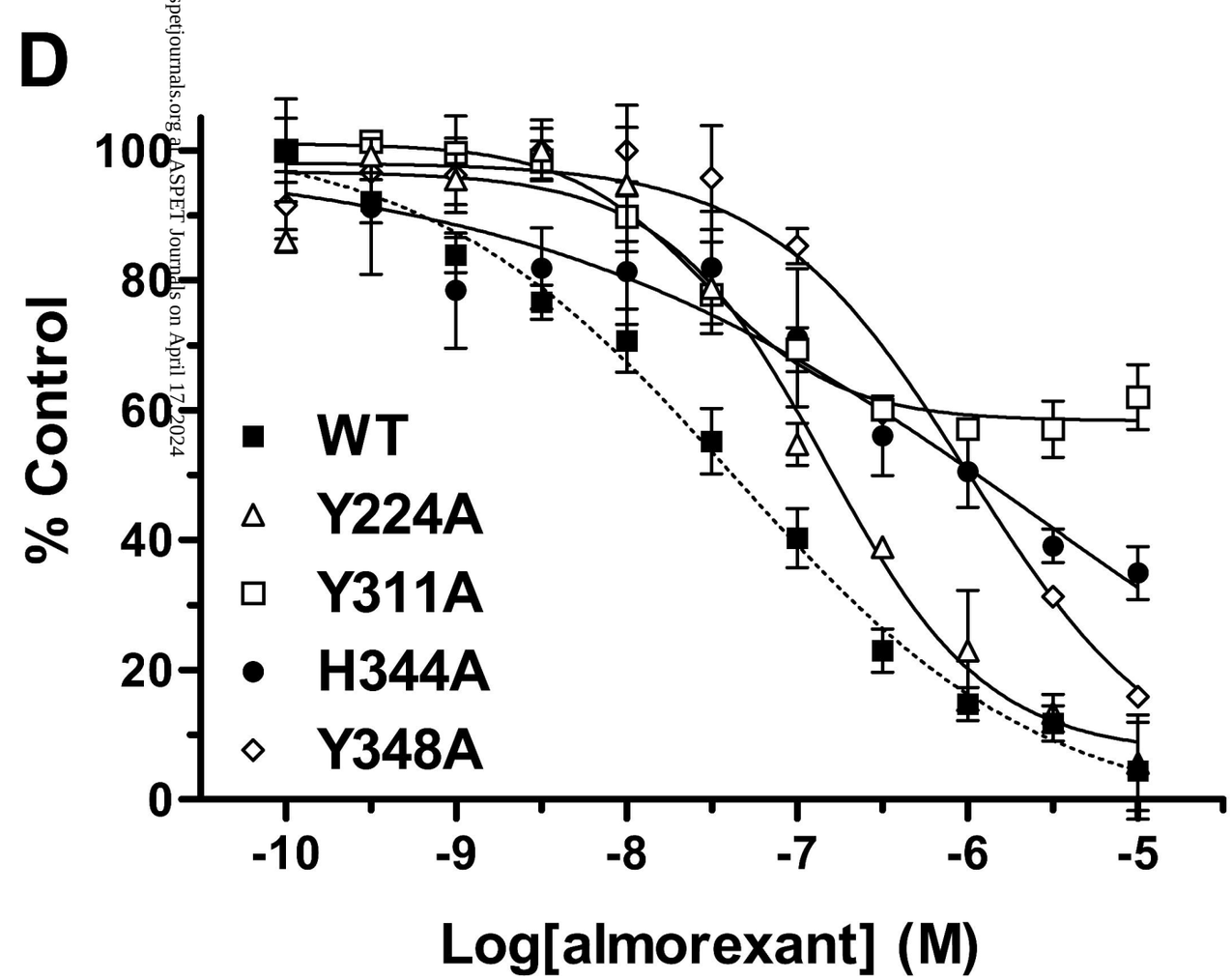

Fig. 5

Fig. 6

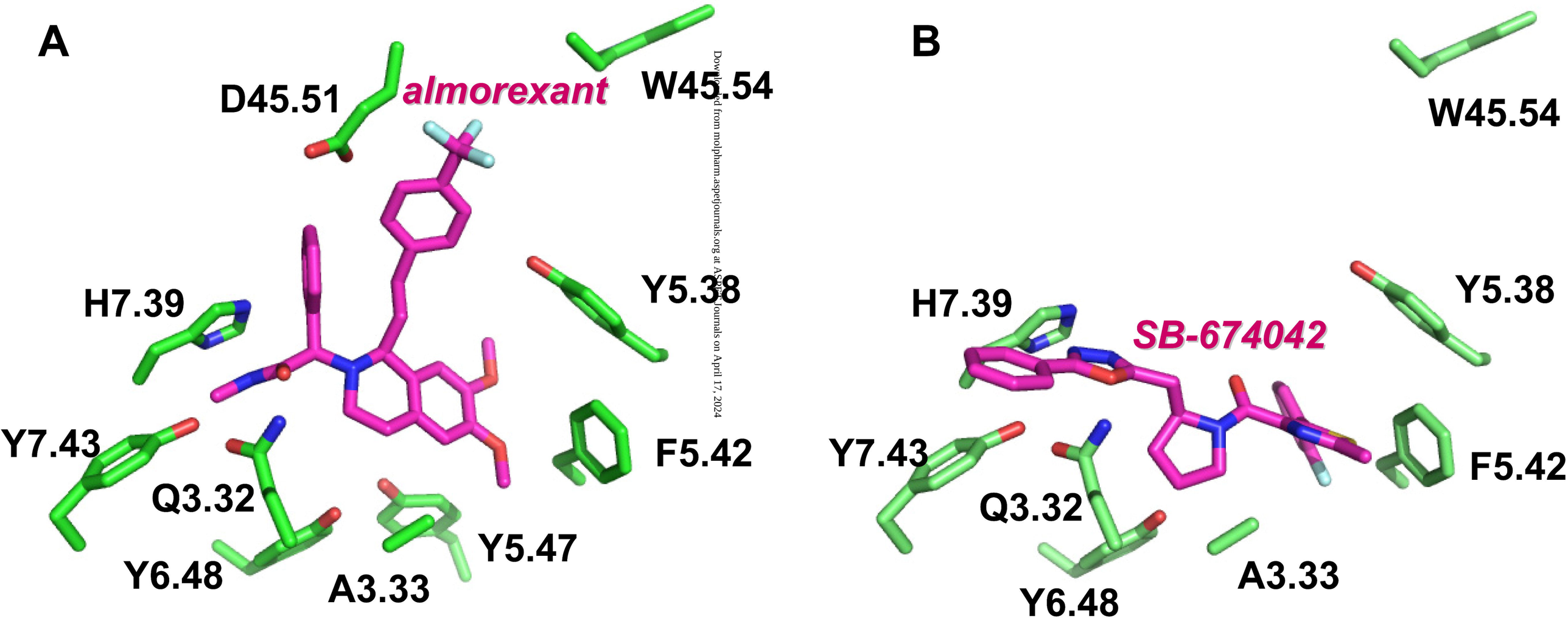

Fig. 7